

Fig. 4. Induction of neuron- and photoreceptor-like cells by treating cells with the combination of 50 μ mol/L taurine and 10 μ mol/L retinoic acid (RA). (A). Procedure for induction of retinal photoreceptor-like cells from NIH/3T3 fibroblasts. Immunocytochemical analysis of β -tubulin (C and E), rhodopsin (G, I, J, K and M) and recoverin (J, L and M) was performed for the treated (E, I, and K-M) and untreated (C, G and J) cells. Phase contrast images of NIH/3T3 cells cultured in NC (B and F) and IM (D and H) were also shown. The percentage of positive cells expressing neuronal or photoreceptor markers is presented in the graph (N). Real-time PCR was carried out to analyze Sox2 (O) and Nestin (P) expression in NSCm-, DM- and IM-cultured cells. The symbols * and ** represent $P < 0.05$ and $P < 0.01$, respectively.

growth factor AA, which was demonstrated to effectively enhance survival of oligodendrocyte progenitors (Yang *et al.* 2005; Chen *et al.* 2007).

Our study demonstrates that NIH/3T3 fibroblasts display some features of neural progenitors and express neuron, astrocyte and even photoreceptor markers under defined conditions. These results shed some light on the induction of retinal photoreceptors from a differentiated cell source. Further studies are necessary to determine if NIH/3T3 fibroblasts can be differentiated into functional neurons or photoreceptors, but the pres-

ent study suggests that neuronal cells can be generated from differentiated cells of other types without the need of adding any epigenetic modifier.

Acknowledgments

This work was supported in part by the Ministry of Health, Labour and Welfare, Japan Foundation for Aging and Health and the Program for Promotion of Fundamental studies in Health Sciences of the National Institute of Biomedical Innovation (NIBIO).

References

- Ahmed, S. 2009. The culture of neural stem cells. *J. Cell. Biochem.* **106**, 1–6.
- Brewer, G. J. & Torricelli, J. R. 2007. Isolation and culture of adult neurons and neurospheres. *Nat. Protoc.* **2**, 1490–1498.
- Chaichana, K., Zamora-Berridi, G., Camara-Quintana, J. & Quinones-Hinojosa, A. 2006. Neurosphere assays: growth factors and hormone differences in tumor and nontumor studies. *Stem cells* **24**, 2851–2857.
- Chen, Y., Balasubramanian, V., Peng, J., Hurlock, E. C., Tallquist, M., Li, J. & Lu, Q. R. 2007. Isolation and culture of rat and mouse oligodendrocyte precursor cells. *Nat. Protoc.* **2**, 1044–1051.
- Chojnacki, A. & Weiss, S. 2008. Production of neurons, astrocytes and oligodendrocytes from mammalian CNS stem cells. *Nat. Protoc.* **3**, 935–940.
- Das, A. V., Mallya, K. B., Zhao, X., Ahmad, F., Bhattacharya, S., Thoreson, W. B., Hegde, G. V. & Ahmad, I. 2006. Neural stem cell properties of Müller glia in the mammalian retina: regulation by Notch and Wnt signaling. *Dev. Biol.* **299**, 283–302.
- Hegde, G. V., James, J., Das, A. V., Zhao, X., Bhattacharya, S. & Ahmad, I. 2007. Characterization of early retinal progenitor microenvironment: presence of activities selective for the differentiation of retinal ganglion cells and maintenance of progenitors. *Exp. Eye Res.* **84**, 577–590.
- Hirami, Y., Osakada, F., Takahashi, K., Okita, K., Yamanaka, S., Ikeda, H., Yoshimura, N. & Takahashi, M. 2009. Generation of retinal cells from mouse and human induced pluripotent stem cells. *Neurosci. Lett.* **458**, 126–131.
- Hoffman, L. M. & Carpenter, M. K. 2005. Characterization and culture of human embryonic stem cells. *Nat. Biotechnol.* **23**, 699–708.
- Holden, C. & Vogel, G. 2008. A seismic shift for stem cell research. *Science* **319**, 560–563.
- Ikeda, H., Osakada, F., Watanabe, K., Mizuseki, K., Haraguchi, T., Miyoshi, H., Kamiya, D., Honda, Y., Sasai, N., Yoshimura, N., Takahashi, M. & Sasai, Y. 2005. Generation of Rx+/Pax6+ neural retinal precursors from embryonic stem cells. *Proc. Natl Acad. Sci. USA* **102**, 11331–11336.
- Jensen, J. B. & Parmar, M. 2006. Strengths and limitations of the neurosphere culture system. *Mol. Neurobiol.* **34**, 153–161.
- Jin, W., Xing, Y. Q. & Yang, A. H. 2009. Epidermal growth factor promotes the differentiation of stem cells derived from human umbilical cord blood into neuron-like cells via taurine induction in vitro. *In Vitro Cell. Dev. Biol. Anim.* **45**, 321–327.
- Klassen, H. & Reubinoff, B. 2008. Stem cells in a new light. *Nat. Biotechnol.* **26**, 187–188.
- Marshall, G. P., Reynolds, B. A. & Laywell, E. D. 2006. Using the neurosphere assay to quantify neural stem cells in vivo. *Curr. Pharm. Biotechnol.* **8**, 141–145.
- Matsuda, N., Lu, H., Fukata, Y., Noritake, J., Gao, H. F., Mukherjee, S., Nemoto, T., Fukata, M. & Poo, M. M. 2009. Differential activity-dependent secretion of brain-derived neurotrophic factor from axon and dendrite. *J. Neurosci.* **29**, 14185–14194.
- Osakada, F., Ikeda, H., Sasai, Y. & Takahashi, M. 2009. Step-wise differentiation of pluripotent stem cells into retinal cells. *Nat. Protoc.* **4**, 811–824.
- Osakada, F., Ikeda, H., Mandai, M., Wataya, T., Watanabe, K., Yoshimura, N., Akaike, A., Sasai, Y. & Takahashi, M. 2008. Toward the generation of rod and cone photoreceptors from mouse, monkey and human embryonic stem cells. *Nat. Biotechnol.* **26**, 215–222.
- Sanchez-Ramos, J., Song, S., Cardozo-Pelaez, F., Hazzi, C., Stedeford, T., Willing, A., Freeman, T. B., Saporta, S., Janssen, W., Patel, N., Cooper, D. R. & Sanberg, P. R. 2000. Adult bone marrow stromal cells differentiate into neural cells in vitro. *Exp. Neurol.* **164**, 247–256.
- Sugano, E., Tomita, H., Abe, T., Yamashita, A. & Tamai, M. 2003. Comparative study of cathepsins D and S in rat IPE and RPE cells. *Exp. Eye Res.* **77**, 203–209.
- Sugano, E., Tomita, H., Ishiguro, S., Abe, T. & Tamai, M. 2005. Establishment of effective methods for transducing genes into iris pigment epithelial cells by using adeno-associated virus type 2. *Invest. Ophthalmol. Vis. Sci.* **46**, 3341–3348.
- Takahashi, K. & Yamanaka, S. 2006. Induction of pluripotent stem cells from mouse embryonic and adult fibroblast cultures by defined factors. *Cell* **126**, 663–676.
- Woodbury, D., Schwarz, E. J., Prockop, D. J. & Black, I. B. 2000. Adult rat and human bone marrow stromal cells differentiate into neurons. *J. Neurosci. Res.* **61**, 364–370.
- Yamanaka, S. 2007. Strategies and new developments in the generation of patient-specific pluripotent stem cells. *Cell Stem Cell* **1**, 39–49.
- Yamanaka, S. 2009. A fresh look at iPS cells. *Cell* **137**, 13–17.
- Yang, Z. S., Watanabe, M. & Nishiyama, A. 2005. Optimization of oligodendrocyte progenitor cell culture method for enhanced survival. *J. Neurosci. Methods* **149**, 50–56.
- Zhang, X. M., Li, Q. M., Su, D. J., Wang, N., Shan, Z. Y., Jin, L. H. & Lei, L. 2010. RA induces the neural-like cells generated from epigenetic modified NIH/3T3 cells. *Mol. Biol. Rep.* **37**, 1197–1202.
- Zhao, X., Liu, J. N. & Ahmad, I. 2002. Differentiation of embryonic stem cells into retinal neurons. *Biochem. Biophys. Res. Commun.* **297**, 177–184.
- Zhou, H., Wu, S., Joo, J. Y., Zhu, S., Han, D. W., Lin, T., Trauger, S., Bien, G., Yao, S., Zhu, Y., Siuzdak, G., Schöler, H. R., Duan, L. & Ding, S. 2009. Generation of induced pluripotent stem cells using recombinant proteins. *Cell Stem Cell* **4**, 381–384.

ORIGINAL ARTICLE

Immune responses to adeno-associated virus type 2 encoding channelrhodopsin-2 in a genetically blind rat model for gene therapy

E Sugano¹, H Isago¹, Z Wang^{1,2}, N Murayama¹, M Tamai³ and H Tomita^{1,4,5}

We had previously reported that transduction of the channelrhodopsin-2 (ChR2) gene into retinal ganglion cells restores visual function in genetically blind, dystrophic Royal College of Surgeons (RCS) rats. In this study, we attempted to reveal the safety and influence of exogenous ChR2 gene expression. Adeno-associated virus (AAV) type 2 encoding ChR2 fused to Venus (rAAV-ChR2V) was administered by intra-vitreous injection to dystrophic RCS rats. However, rAAV-ChR2 gene expression was detected in non-target organs (intestine, lung and heart) in some cases. ChR2 function, monitored by recording visually evoked potentials, was stable across the observation period (64 weeks). No change in retinal histology and no inflammatory marker of leucocyte adhesion in the retinal vasculature were observed. Although antibodies to rAAV (0.01–12.21 $\mu\text{g ml}^{-1}$) and ChR2 (0–4.77 $\mu\text{g ml}^{-1}$) were detected, their levels were too low for rejection. T-lymphocyte analysis revealed recognition by T cells and a transient inflammation-like immune reaction only until 1 month after the rAAV-ChR2V injection. In conclusion, ChR2, which originates from *Chlamydomonas reinhardtii*, can be expressed without immunologically harmful reactions *in vivo*. These findings will help studies of ChR2 gene transfer to restore vision in progressed retinitis pigmentosa. Gene Therapy advance online publication, 28 October 2010; doi:10.1038/gt.2010.140

Keywords: retinitis pigmentosa; channelrhodopsin-2; immunoreactivity; adeno-associated virus; retinal ganglion cells

INTRODUCTION

Retinitis pigmentosa (RP) is a group of diseases in which a gene mutation results in the death of photoreceptor cells. At present, approximately 40 genes have been identified as the causative agents (<http://www.sph.uth.tmc.edu/retnet/>; provided in the public domain by the University of Texas Houston Health Science Center, Houston, TX, USA). The initial visual impairment in patients with RP is night blindness, and patients lose their vision in the final stage of this disease following visual field loss.¹ Many trials have been conducted to identify agents that can protect photoreceptors and delay vision loss, but effective treatments have not been developed against progressed RP.

Although photoreceptor cells are often degenerated in the case of progressed RP, other inner neurons, including retinal ganglion cells (RGCs) are preserved.² It would be ideal to utilise the remaining retinal neurons to restore vision. We have been studying light-gated cation-selective membrane channel protein channelrhodopsin-2 (ChR2)³ to induce photoreceptor function in retinal neurons such as RGCs^{4,5} and ON bipolar cells.⁶ We have already demonstrated that the responses induced by various stimulus frequencies (Hz) in ChR2-transduced rats are in no way inferior to those in normal rats,⁷ as supported by the finding that ChR2-induced photocurrents are extremely fast.^{8,9} Visual function was also well analysed by using transgenic rats with ChR2 transduction into RGCs: the spatial

frequencies based on behavioural responses of photoreceptor-degenerated ChR2 transgenic rats were the same as those of normal rats.¹⁰ These studies indicate that transfer of the ChR2 gene into the remaining retinal neurons is a useful method for restoring vision in progressed RP.

However, for clinical application of ChR2 therapy, some problems must be considered. First, this approach is a gene therapy. An immune response (mostly a problem with adenovirus- and herpes simplex virus-derived vectors)¹¹ may be caused by adeno-associated virus (AAV) and its incorporation into the host genome may lead to de-repression of tumour suppression genes.^{12–14} Second, ChR2 is a protein originating from *Chlamydomonas reinhardtii*. It is important to study the systemic responses on virus vector application and long-term expression of the transgene product in humans. In this study, to reveal the safety and influence of exogenous ChR2 gene expression, we investigated the functional stability of the ChR2 gene and the possibility of harmful immune reactions caused by this gene therapy in a Royal College of Surgeons (RCS) rat model of RP.

RESULTS

Recording of visually evoked potentials (VEPs) in RCS rats

Although RGCs are maintained in aged RCS (*rdy/rdy*) rats, VEPs would be abolished because of the loss of light-evoked synchronous activities by photoreceptor cells. Indeed, VEPs were not evoked even

¹Department of International Advanced Interdisciplinary Research, Institute for International Advanced Research and Education, Tohoku University, Sendai, Japan; ²Japan Foundation for Aging and Health, Aichi, Japan; ³School of Medicine, Tohoku University, Sendai, Japan; ⁴United Centers for Advanced Research and Translational Medicine, School of Medicine, Tohoku University, Sendai, Japan and ⁵Innovation of New Biomedical Engineering Center, Tohoku University, Sendai, Japan

Correspondence: Dr H Tomita, Department of International Advanced Interdisciplinary Research, Institute for International Advanced Research and Education, Tohoku University, 4-1 Seiryō-machi, Aoba-ku, Sendai 980-8575, Japan.

E-mail: hiroshi-tomita@iare.tohoku.ac.jp

Received 9 June 2010; revised 29 August 2010; accepted 7 September 2010

by the maximum flash of the light-emitting diode in any of the 6-month-old RCS (*ryd/ryd*) rats. After confirmation of the loss of photoreceptor-derived function, AAV encoding ChR2 fused to Venus (rAAV-ChR2V) was administered by intra-vitreous injection into the left eye. The right eye was not treated and served as the control. At 2 weeks after the injection, VEPs were recorded in the right visual cortex. The amplitude peaked at 8 weeks but remained stable until 64 weeks after the injection (Figure 1). There was no recording from the left side of the visual cortex (data not shown). We could not record for longer periods than 64 weeks because the lifespan of RCS rats is about 2 years.

Viral dissemination to the organs

To determine systemic dissemination of rAAV after the injection, total ribonucleic acids were isolated from each organ after 6 months of rAAV-ChR2V administration. No rAAV-derived Venus expression was

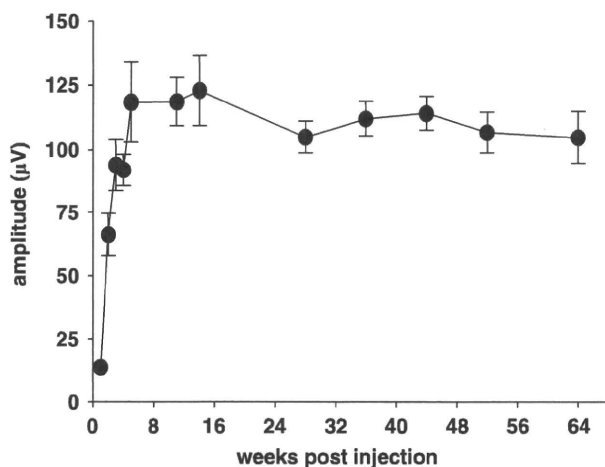


Figure 1 Long-term functional analysis of photosensitivity following ChR2 gene transfer by intra-vitreous injection of rAAV-ChR2V in 6-month-old RCS (*ryd/ryd*) rats. A blue LED (wavelength, 435–500 nm; peak, 470 nm) was flashed for 20 ms at 2.6 mW cm^{-2} and time-dependent improvements in the amplitude of the VEPs were recorded. After peaking at 8 weeks of administration, the amplitude remained stable for 64 weeks post-injection.

detected by reverse transcription-polymerase chain reaction (RT-PCR) analysis from the brain, liver, spleen and kidney (Figure 2). As expected, we detected the appropriate Venus protein expression from the rAAV-transduced retinas. Venus expression was unexpectedly detected in other organs (heart, lung and intestine) in some cases.

Histological examination of rAAV-ChR2V-treated retina

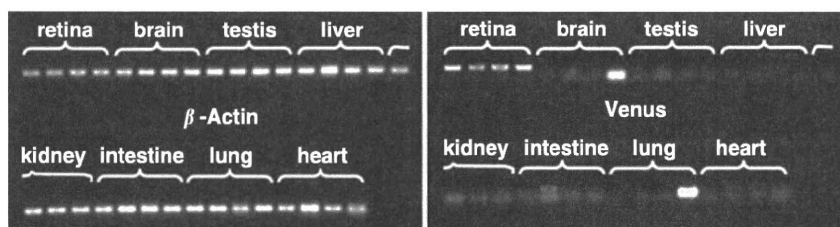
The rAAV-derived gene expression was investigated by observing whole-mounted retina. At 6 months after rAAV administration, the expression of ChR2V or Venus was observed by fluorescence microscopy (Figure 3). ChR2V was expressed in the plasma membrane of the retinal cells; on the other hand, Venus expression was observed in the cytoplasm of the rAAV-Venus-injected retina. Both of the rAAV-derived proteins were expressed all over the retina, and there was some deflection of the retinal expression.

To assess the side effects of ChR2 gene transfer by using rAAV, histological studies were performed on paraffin-embedded and frozen sections. There was no obvious difference in the retinal morphology between the ChR2-injected and the age-matched untreated RCS (*ryd/ryd*) rats (Figures 4a and b). However, intra-vitreous injection of lipopolysaccharide, which resulted in endotoxin-induced uveitis (EIU), in the RCS (+/+) rats caused substantial migration of inflammatory cells, mainly polymorphonuclear leucocytes, in the neural retina and vitreous humour (Figure 4d).

When the retinal activities were studied in frozen sections by immunohistochemistry (Figure 5), glial fibrillary acidic protein (GFAP) expression was restricted to the ganglion cell layers in the rAAV-ChR2V-treated retina (Figure 5c); however, GFAP expression was observed throughout the inner half of the retina in the untreated RCS (Figure 5b) and rAAV-Venus-injected RCS (Figure 5d) rats. Nuclear factor- κ B (NF- κ B) expression was restricted to the ganglion cell layers in all the tested RCS rats, but it was markedly high in the rAAV-ChR2V-treated retinas (Figure 5h).

Effects of rAAV-ChR2V treatment on leucocyte adhesion in the retinal vasculature

The retinal adherent leucocytes were imaged by perfusion labelling with fluorescein isothiocyanate-coupled concanavalin A. According to a report of Koizumi *et al.*,¹⁵ leucocyte adhesion is significantly elevated



The expression of venus protein, which was carried by rAAV

	retina	brain	testis	liver	kidney	intestine	lung	heart
Sample1	+++	-	-	-	-	-	-	-
Sample2	+++	-	-	-	-	++	-	+
Sample3	+++	-	-	-	-	-	-	+
Sample4	+++	-	-	-	-	-	+	+

Abbreviations : -, No expression; +, Light expression; ++, Moderate expression; +++, Intense expression;

Figure 2 Virus dissemination to the organs. At 6 months after the administration of rAAV-ChR2V, total ribonucleic acid was extracted from the retina, brain, testis, liver, kidney, intestine, lung and heart. The rAAV-derived gene was investigated by using RT-PCR analysis. As expected, a high copy number of the rAAV-derived gene expression was detected in the retina. The gene expression was also detected in the heart, lung and intestine in some cases.

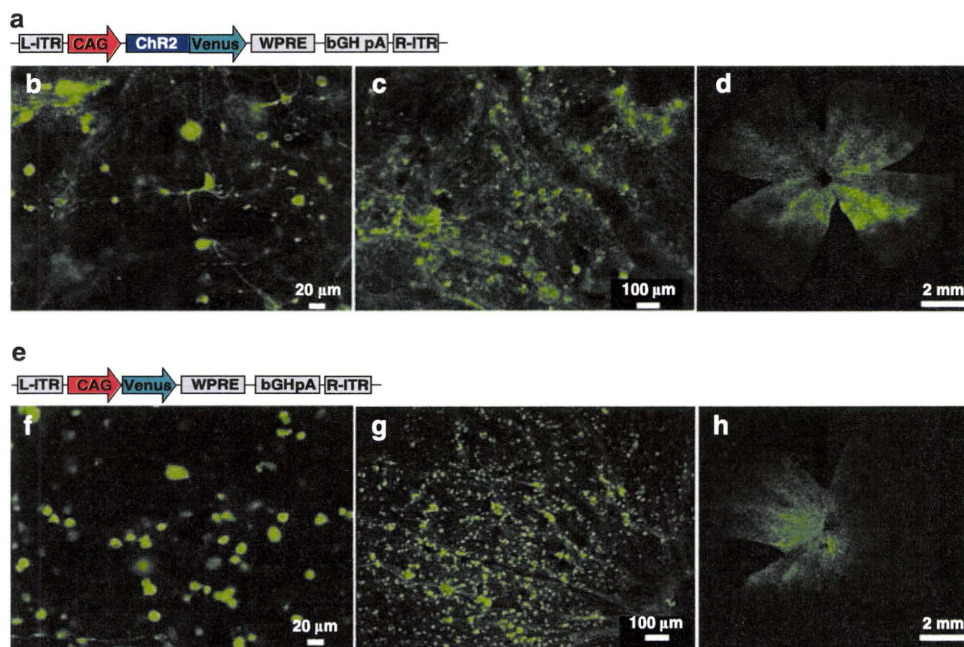


Figure 3 Expression profiles of the rAAV-derived proteins in the retina. Construction of the rAAV vector expressing ChR2V (a) and Venus (e) is illustrated. After 6 months of intra-vitreous injection, the rAAV-derived protein expression in whole-mounted retinal samples was observed by fluorescence microscopy. ChR2V expression was observed in the membrane (b–d) and Venus was expressed in the cytoplasm (f–h) of the retinal cells.

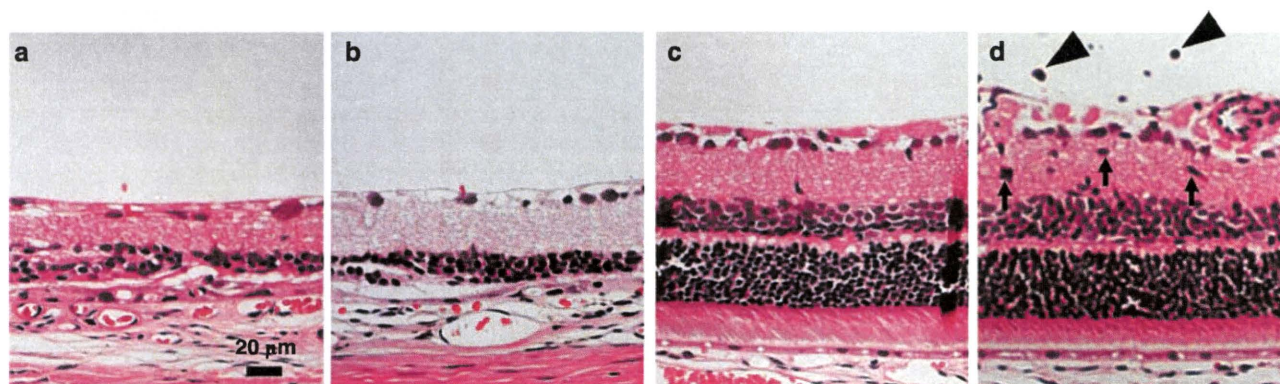


Figure 4 Histological examination of rAAV-ChR2V-treated retina. rAAV-ChR2V was administered by intra-vitreous injection into the left eye of RCS (*rdylr/dy*) rats. After 64 weeks, their right (control) (a) and left (b) eyeballs were enucleated and stained with hematoxylin and eosin. As a model of inflammation, age-matched RCS (+/+) rats were administered lipopolysaccharide (LPS) by intra-vitreous injection and their eyeballs were enucleated after 48 h. Retinal sections of untreated RCS (+/+) (c) and the LPS-treated (d) rats were studied. Substantial infiltration of inflammatory cells, which were mainly PMNLs in the neural retina (arrow) and vitreous humour (arrowhead), was observed in the retina of the LPS-treated rats.

after the development of EIU. Our study demonstrated that EIU caused leucocyte adhesion in the retinal venules (Figures 6c and d). However, there was no difference in leucocyte adhesion between the untreated (Figure 6a) and the rAAV-ChR2V-injected (Figure 6b) RCS rats, which had received the rAAV injection 1 year previously.

Humoral immune responses to the viral vector and transgene

To assess the possibility of a systemic humoral immune response to the viral vector or transgene, we determined the antibody levels against the rAAV2 capsid and ChR2 in serum by enzyme-linked immunosorbent assay. In the rAAV-ChR2V-injected rats, rAAV2 capsid-specific antibodies were detected and showed the maximum production at 2 months after injection ($0.01\text{--}12.21\ \mu\text{g ml}^{-1}$;

Figure 7a). However, the titre was extremely low in this study compared with that in a previous report of intramuscular injection of AAV2 ($200\text{--}400\ \mu\text{g ml}^{-1}$).¹⁶ The titre against the ChR2 protein was the maximum at 6 months post-injection. However, this level was also low ($0\text{--}4.77 \pm 2.55\ \mu\text{g ml}^{-1}$) compared with the antibody level in serum of the immunized rabbit ($1442.34\ \mu\text{g ml}^{-1}$), which received a peptide injection to produce antibody to ChR2 forcibly (Figure 7b).

Analysis of T-lymphocyte subsets

Total T lymphocytes were gated with positive staining of anti-CD3. Then, the population of lymphocytes was confirmed by forward scatter (cell size) versus side scatter (cell granularity). Analysis of T lymphocyte subsets, namely CD4⁺ (T helper cells), CD8⁺ (cytotoxic

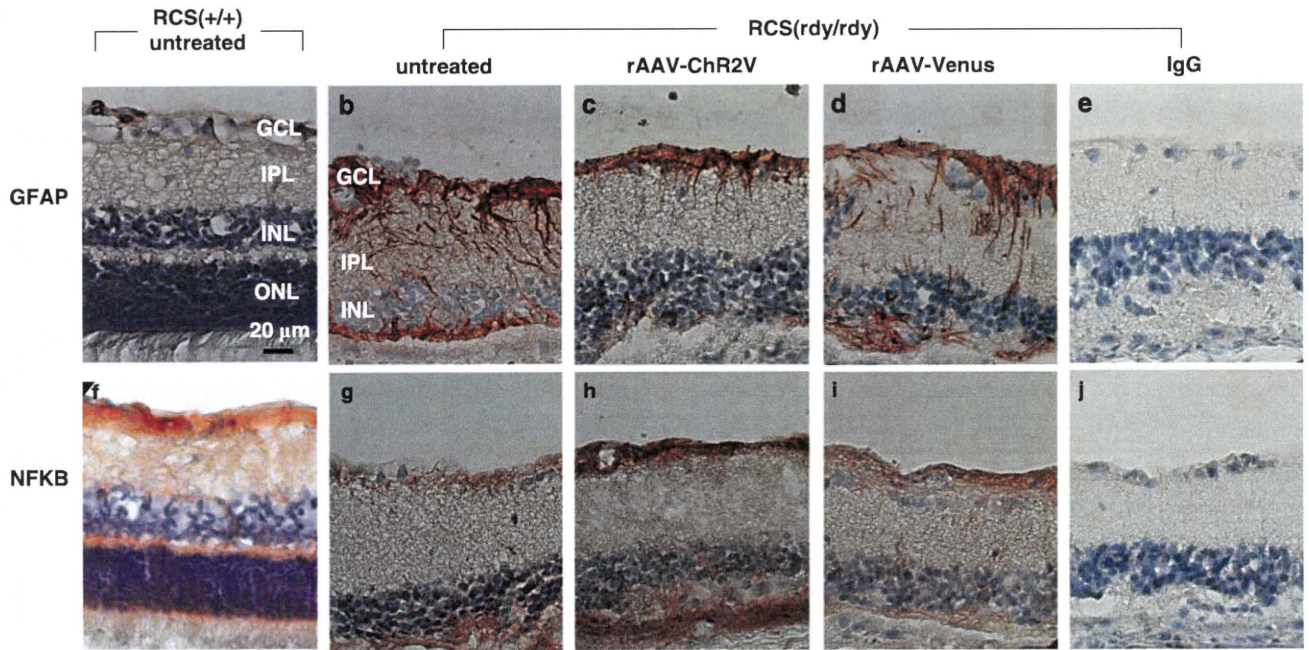


Figure 5 Changes in the protein immunoreactivities in the retina. Untreated RCS (+/+) (a and f) and RCS (*rdy/rdy*) (b and g) rats were used as the controls. rAAV-Venus (d and i) or rAAV-ChR2V (c and h) was administered by intra-vitreous injection into the left eye of RCS (*rdy/rdy*) rats. After 64 weeks, their eyeballs were enucleated. All the RCS rats were of the same age at the time of enucleation (2.2 years). As the negative control for staining, the first antibodies were replaced with non-immune mouse immunoglobulin G (e and j). DNA was counterstained with 4', 6-diamidino-2-phenylindole. GFAP expression was restricted to the ganglion cell and nerve fibre layers of the ChR2V-treated retina (c); however, it was observed throughout the inner half of the retina in the untreated RCS (b) and rAAV-Venus-injected RCS (d) rats. Nuclear factor- κ B expression was restricted to the ganglion cell layers in all the tested RCS rats, but it was markedly high in the ChR2V-treated retina (h).

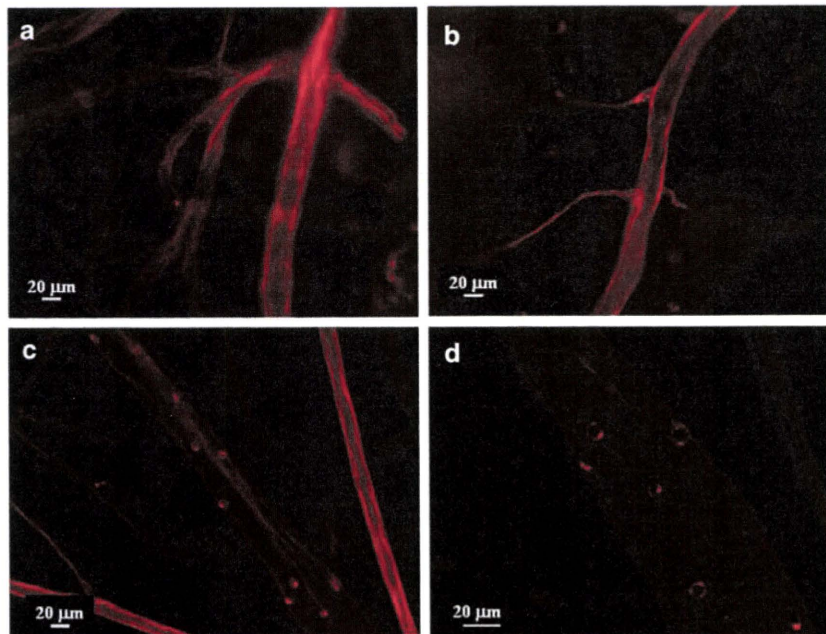


Figure 6 Adverse effect of rAAV-ChR2V treatment on retinal leucocyte adhesion. To study the adverse effect of ChR2 treatment in RCS rats, their retinas were examined after 1 year of rAAV-ChR2V injection. As a model of inflammation, RCS (+/+) rats received an intra-vitreous injection of lipopolysaccharide (LPS) and were examined 48 h after the injection. Flat-mounted retinas labelled with concanavalinA lectin showed increased number of adherent leucocytes in the retinal vessels of the LPS-injected rats (c) compared with the untreated (a) and rAAV-ChR2V-injected (b) rats. High-magnification photography of the LPS-treated retinal vessels showed leucocyte adhesion more clearly (d).

cells) and CD4⁺CD25⁺ (T regulatory cells), was performed. The CD4⁺/CD8⁺ ratio is a known indicator of the immunoregulatory status.^{17,18} Our results demonstrated that the CD4⁺/CD8⁺ ratio after

1 week of the rAAV injection was higher than the pre-injection ratio (Figure 8a). This increase occurred in the case of both the rAAV-Venus and rAAV-ChR2V injections. In addition, the CD4⁺/CD8⁺ ratio only 1

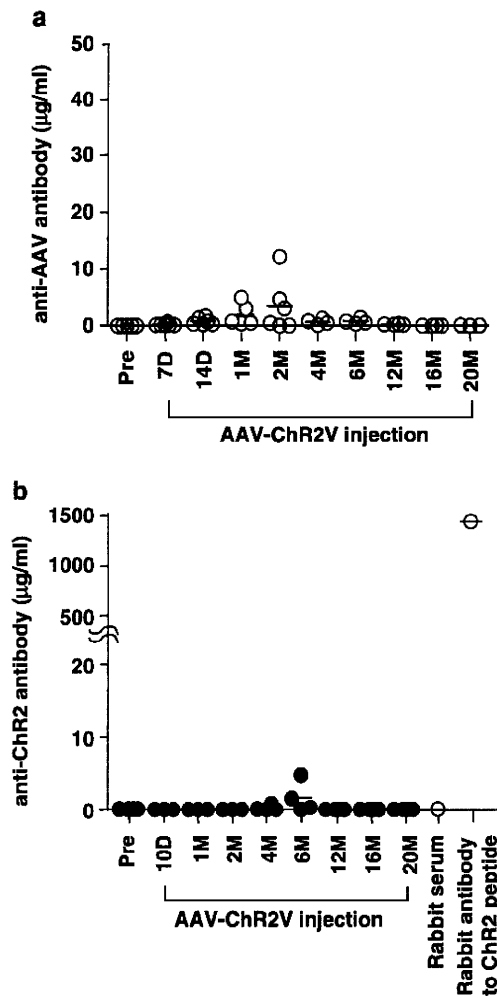


Figure 7 Humoral immune responses to the viral vector and transgene. Production levels of the antibodies to the AAV2 vector (a) and the therapeutic gene, ChR2 (b), were studied in RCS rats following a single intra-vitreous injection of rAAV-ChR2V. The time after injection is indicated. The antibody levels against both AAV2 and ChR2 were quite low compared with the antibody levels in serum of an immunized rabbit, which were considered as the effective dose to react with antigens.

month after the rAAV-ChR2V injection was higher than that before the injection. These data suggested that a change in the inflammation status occurred from 1 week to 1 month after rAAV administration. After this period, the ratios decreased to the pre-injection value and were stable for 1 year. To assess the inflammation status, we studied T regulatory cells. As shown in Figure 8b, a significant increase in the number of CD4⁺CD25⁺ cells was observed at 1 week after the rAAV-Venus and rAAV-ChR2V injections compared with the numbers before the injections. There was no significant difference in the inflammation status between the rAAV injections. As a positive control of inflammation, EIU also increased the population of CD4⁺CD25⁺ cells, which is consistent with a report by Toda *et al.*¹⁹

DISCUSSION

The results of this study demonstrate that the strategy of restoration of vision and light responses in photoreceptor-degenerated RCS (*rdy/rdy*) rats by rAAV-ChR2V administration was technically feasible and safe. Most importantly, ChR2 function, which was confirmed by

measuring VEPs, was not reduced over the whole observation period after rAAV-ChR2V administration (Figure 1). A single administration of rAAV-ChR2V restored the light sensitivity over the lifespan of the rat model.

The eye is considered to be an immunologically protected space.²⁰ This immune privilege is the result of multiple layers and mechanisms, including the blood–retina barrier and other physical barriers, such as the immunosuppressive microenvironment against deviant systemic immunity, that limit the production of pro-inflammatory effector cells. We predicted that systemic dissemination of a virus would be limited by these immune systems after intra-vitreous injection. To investigate the systemic dissemination of rAAV, ribonucleic acids were isolated from each organ and the expressions of the Venus protein, which was fused to rAAV-ChR2, were studied (Figure 2). Venus expression was notable in the retina. Contrary to our expectations, the expression was also detected in the intestine, lung and heart in some cases. The RCS (*rdy/rdy*) animal model, which genetically causes loss of photoreceptors, is reported to have some breakdown of the blood–retina barrier or other mechanisms.^{21–24} Therefore, the rAAV vector might have been disseminated to the other organs. Supporting this hypothesis, the efficiency of rAAV-derived gene transfer was higher in RCS rats than in normal rats (data not shown). This result suggests that some breakdown of the retinal barriers increased the permeability to rAAV.

The genomes transferred by rAAV tend to persist in cells mainly in an episomal, non-integrated form.²⁵ The transferred genomes in episomal form are diluted by cell division. However, when rAAV-carried genomes are inserted into chromosomes of cells with high proliferation ability, the genomes are preserved. There were some differences in gene delivery by rAAV among the samples obtained from the intestine, lung and heart. These differences might be the result of differences in the insertion forms of the rAAV genomes.

In gene therapy, tumour formation caused by the insertion of a transgene into the genome has been reported.^{12–14} We did not observe tumour formation in any of the rats that received the rAAV injections (data not shown). For more information regarding tumour formation, further studies are needed by using methods such as Northern blotting, integration site analysis²⁶ and oncogene analysis.

We also investigated the inflammatory responses caused by the gene transfer by using the EIU model as a positive control of inflammation. EIU caused ocular inflammation, including leucocyte infiltration into the vitreous humour (Figure 4d) and leucocyte adhesion to the retinal vessels (Figures 6c and d). These findings are consistent with those of previous reports.^{15,27} However, we did not observe such inflammatory cells in the retinas treated with rAAV-Venus or rAAV-ChR2V. Therefore, rAAV-ChR2V administration did not induce inflammation arising from bacterial infection.

GFAP is reportedly expressed because of gliosis and hypertrophy of macroglial cells.²⁸ Moreover, GFAP is expressed in astrocytes in the retina usually, but in Müller cells under pathological or stress conditions.²⁹ GFAP was also reported to be upregulated in the brain astrocytes during the inflammatory response.³⁰ Beurel and Jope³¹ revealed that GFAP upregulation is caused by the production of the inflammatory cytokine interleukin-6. The absence of GFAP upregulation by viral injection (Figures 5b–d) demonstrates the lack of glial activation derived from inflammation. Our study showed that GFAP was expressed throughout the retina in the untreated RCS rats and that the expression was decreased and restricted by the rAAV-ChR2V injection (Figure 5c). These results reveal that activation of RGCs by ChR2 may have a protective effect on the inner retina.^{32,33} NF-κB expression in the retina was restricted to the ganglion cell layers in all

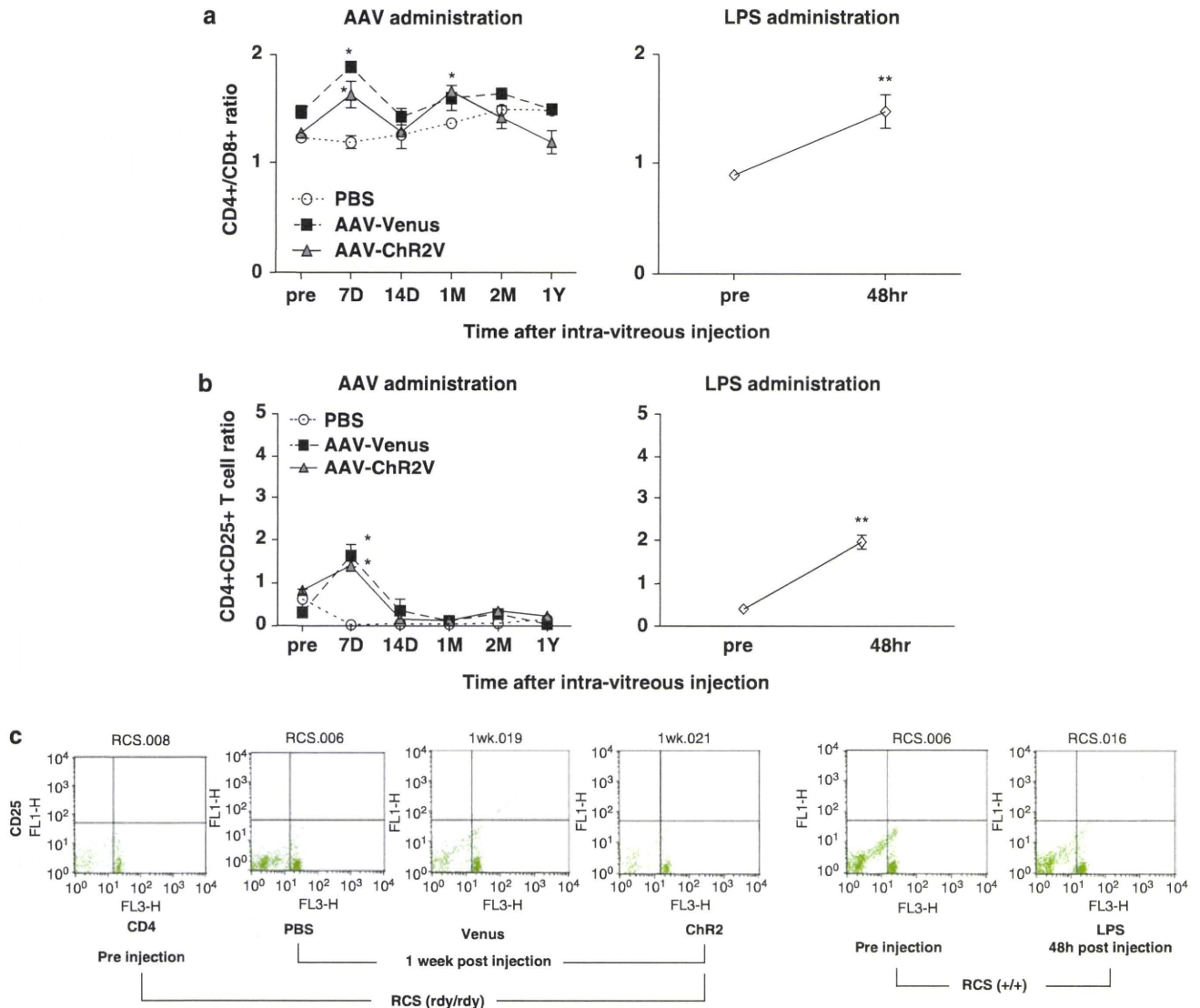


Figure 8 T-cell ratio in the peripheral blood. Lymphocytes were isolated from the peripheral blood before and after injection of PBS, rAAV-Venus or rAAV-ChR2V. The lymphocytes were incubated with anti-T-cell receptor-associated CD3, anti-CD4 and anti-CD8a mAbs, and analysed by flow cytometry. The blood of lipopolysaccharide-administrated rats as a positive control of inflammation was also analysed. The T-cell ratio of CD4⁺/CD8⁺ (a) and CD4⁺CD25⁺ (T regulatory cells) (b) was calculated. (c) Representative data of T regulatory analysis are indicated. All data are represented as the mean (s.d.) of four to seven animals.

the experiments and there was no staining of the other inner retinal cells, which was caused by stress.³⁴ We also demonstrated the potent expression of NF- κ B p65 in the rAAV-ChR2V-injected retinas. These results are consistent with reports that constitutive NF- κ B activity is the result of ongoing synaptic activity.^{35,36}

The T-lymphocyte analysis demonstrated that the CD4⁺/CD8⁺ ratio was higher in all the rAAV-treated rats at 1 week after the injection than before the injection, and in the rAAV-ChR2V-treated rats, the ratio was high at 1 month after injection (Figure 8a). However, these increases were transient and returned to the pre-injection level. This expansion allows cross-talk between different types of cells in the ongoing immune response.¹⁷ Kim and Lim¹⁸ reported that CD4⁺/CD8⁺ expansion is caused by bacterial infection. After 1 week, the ratio increased in all the rAAV-injected rats. Thus, there might have been some immune reactions such as antigen presentation to rAAV. At 1 month after the rAAV-ChR2V injection, the ratio increased

again. As shown in Figure 1, the maximum ChR2 function was recorded at 1 month in the visual cortex first. Thus, some immune reactions might have been induced by increased ChR2 expression but were well tolerated at 2 months after the injection.

Currently, the best characterized regulatory cells are CD4⁺CD25⁺ T cells.³⁷ These cells can suppress host immune responses and modulate the immune responses in autoimmune diseases, allergy, transplantation and infectious diseases.^{38,39} CD25, an interleukin-2 receptor, is reported to be an inflammation marker on CD4⁺ lymphocytes.¹⁸ In the EIU experiment, we observed expansion of CD4⁺CD25⁺ cells, which is consistent with the report by Toda *et al.*¹⁹ A significant increase in the number of CD4⁺CD25⁺ cells was observed in both the rAAV-Venus and the rAAV-ChR2V rats at 1 week after the injections compared with the pre-injection values (Figure 8b), although there was no significant difference in the results between the rAAV-Venus and the rAAV-ChR2V injections.

These results demonstrate that the inflammation-like immunological reaction was caused by AAV and not by Chr2.

To assess the possibility of a systemic humoral immune response to the viral vector or transgene product, we measured the antibody levels of the rAAV2 capsid and Chr2 in serum by enzyme-linked immunosorbent assay. Intra-vitreous injection caused relatively little antibody production (Figure 7a) compared with the different route of AAV injection used by Zhang *et al.*¹⁶ Li *et al.*⁴⁰ demonstrated that a single intra-vitreous injection of AAV2 causes increased AAV antibody production at 2 months after injection. Our data are consistent with their report in terms of the timing of increase and the amount of antibody production (Figure 7a). We anticipated that Chr2 expression would cause antibody production because Chr2 is not inherent to humans. However, the production levels were relatively low (Figure 7b) and were insufficient to induce a humoral immune response.

In conclusion, an immune reaction can be caused by AAV administration and Chr2 protein expression, but will be well tolerated. It should be noted that the experiments were performed in rats and cannot be directly extrapolated to humans, who constitute a far more immunologically heterogeneous population. However, these findings will help studies of Chr2 gene transfer to restore vision in progressed RP.

MATERIALS AND METHODS

Animals

In total, 59 (6-month-old male) RCS rats (43 dystrophic (*rdy/rdy*)); 16 non-dystrophic (+/+) were used in this study (Table 1). The animals were maintained and used in accordance with the ARVO Statement for the *Use of Animals in Ophthalmic and Vision Research and the Guidelines for Animal Experiments of Tohoku University*. All the animal experiments were conducted with the approval of the Animal Research Committee, School of Medicine, Tohoku University. To compare the functions, the control and treated rats were age-matched in each experiment.

Induction of EIU

As a model of ocular inflammation,⁴¹ RCS (+/+) rats received a single intra-vitreous injection of 5 µg lipopolysaccharide from *Escherichia coli* (055:B5; Sigma, St Louis, MO, USA) in 5 µl phosphate-buffered saline (PBS) to cause

EIU. After 48 h of lipopolysaccharide administration, the inflammation status was studied.

Preparation of AAV vector carrying the Chr2 gene construct

The N-terminal fragment (residues 1–315) of Chr2 (GenBank accession no. AF461397) was fused to a fluorescent protein, Venus, in frame at the end of the Chr2-coding fragment described previously.⁵ The Chr2V or Venus gene was introduced into the *EcoRI* and *HindIII* sites of the 6P1 plasmid.⁴² The synapsin promoter was exchanged for a hybrid cytomegalovirus enhancer/chicken β-actin promoter,⁴² and AAV-Chr2V and AAV-Venus were constructed. The pAAV-RC and p-Helper plasmids were obtained from Stratagene (La Jolla, CA, USA). Semi-confluent 293T cells on 15-cm plates were co-transfected with split-packaging plasmids—AAV-Chr2V (or AAV-Venus), pAAV-RC and p-Helper—by using a calcium phosphate-based protocol according to the manufacturer's instructions (Agilent Technologies, La Jolla, CA, USA). The rAAV vectors (rAAV-Chr2V, rAAV-Venus) were purified by using the method of Auricchio *et al.*^{43–45}

rAAV vector injection

The rAAV-Chr2V or rAAV-Venus vector was administered by intra-vitreous injection into the left eye of 6-month-old RCS (*rdy/rdy*) rats. In brief, the rats were anaesthetised by intramuscular injection of a mixture of ketamine (66 mg ml⁻¹) and xylazine (33 mg kg⁻¹). Under an operating microscope, the conjunctiva was incised to expose the sclera. A total volume of 5 µl of vector suspension at a concentration of 5 × 10¹² genomic particles per µl was administered by intra-vitreous injection through the ora serrata with a 10-µl Hamilton syringe and a 32-gauge needle (Hamilton Company, Reno, NV, USA).

Recording of VEPs

VEPs were recorded by using Neuropack MEB-9102 (Nihon Kohden, Tokyo, Japan). The method of recording was derived from a combination of protocols used by Papathanasiou *et al.*⁴⁶ and Iwamura *et al.*⁴⁷ In brief, at least 7 days before the experiments, recording electrodes (silver–silver chloride) were placed epidurally on each side 7 mm behind the bregma and 3 mm lateral to the midline, and a reference electrode was placed epidurally on the midline 12 mm behind the bregma. Under ketamine–xylazine anaesthesia, the pupils were dilated with 1% atropine and 2.5% phenylephrine hydrochloride. The ground electrode clip was placed on the tail. Photostimuli of 20-ms duration were applied at a frequency of 0.5 Hz and generated by pulse activation of a blue light-emitting diode with light-emitting wavelengths in the range 435–500 nm (peak, 470 nm). A total of 100 consecutive response waveforms were averaged for the VEP measurements.

Table 1 The Number of samples examined in this study

	VEP	PCR	Expression in retina (whole mount)	Histology (HE)	Immuno- histochemistry	Leukocyte adhesion	Antibody detection	Flow cytometry	Total (n)
No treatment (+/+)				3	3	3			9
Pre-treatment (+/+)								7	7
LPS administration (+/+)				3		4		7	
No treatment (<i>rdy/rdy</i>)				3	3	3			9
Pre-injection for PBS (<i>rdy/rdy</i>)								4	4
After PBS injection (<i>rdy/rdy</i>)								4	
Pre-injection for rAAV-Venus (<i>rdy/rdy</i>)								4	10
After rAAV-Venus injection (<i>rdy/rdy</i>)			3		3			4	
Pre-injection for rAAV-Chr2V (<i>rdy/rdy</i>)	20						3–6	4	20
After rAAV-Chr2V injection (<i>rdy/rdy</i>)	20	4	3	3	3	3	3–6	4	

Abbreviations: Chr2V, channelrhodopsin-2 fused to Venus; HE, hematoxylin and eosin; LPS, lipopolysaccharide; PBS, phosphate-buffered saline; PCR, polymerase chain reaction; rAAV, adeno-associated virus type 2; VEP, visually evoked potential.

Ribonucleic acid isolation and rAAV-derived protein detection by RT-PCR analysis

Total ribonucleic acids were extracted (TRIreagent; Sigma) from the retina, brain, lung, testis, liver, kidney, intestine, lung and heart. cDNA was synthesised (First-Strand cDNA synthesis kit; GE Healthcare, Piscataway, NJ, USA) and the tracer fusion protein, Venus, expression was investigated by using a semi-quantitative RT-PCR method. As the individual internal control, we performed PCR with β -actin. The primer sequences were as follows: 5'-TCATGAAGTGTGACGTTGACATCCGT-3' (sense) and 5'-CCTAGAAGCATTTCGGGTGCACGATG-3' (antisense) for β -actin; 5'-GACGTAAACGGCCACAAGTT-3' (sense) and 5'-GAACTCCAGCAGGACCATGT-3' (antisense) for Venus. Following electrophoresis on 1.0% agarose gel, DNA was detected by staining with GelRed (Biotium, Inc., Hayward, CA, USA).

Histology

After death, the eyeballs were enucleated, immersed in 4% paraformaldehyde in PBS overnight at 4 °C and embedded in paraffin. Serial sections (4 μ m) of whole eyes were cut sagittally, through the cornea and parallel to the optic nerve, and stained with haematoxylin and eosin. Microscopic examination of the sections was then performed (AxioImager A1; Carl Zeiss, Tokyo, Japan).

The Chr2V expression profile in the retina was studied according to the method we previously described.⁵ In brief, the eyes were fixed and the retinas were flat-mounted on slides. Venus fluorescence was visualised under a fluorescence microscope (BZ-9000; Keyence Corp., Osaka, Japan).

Immunohistochemistry

Rat eyes were fixed overnight at 4 °C in 4% paraformaldehyde in PBS (pH 7.4). The retinas were rinsed with PBS and immersed in 10, 20 and 30% sucrose in PBS at 4 °C. Samples were embedded in optimal cutting temperature compound (Sakura, Tokyo, Japan) under liquid nitrogen and stored at -80 °C. Cryosections (10 μ m) of tissue were mounted on slides and air dried. Then, retinal sections were washed with PBS and treated for 15 min with 0.3% H₂O₂ in methanol. After washing with PBS, the sections were incubated with mouse anti-rat NF- κ B p65 (C-20) antibody (1:200; Santa Cruz Biotechnology, Santa Cruz, CA, USA) and mouse anti-rat GFAP antibody (1:250; Nihon Millipore, Tokyo, Japan) in antibody diluent buffer (0.05% Tween-20, 3% bovine serum albumin and 3% goat serum in PBS) overnight at 4 °C. After washing with 0.05% Tween-20 in PBS, the sections were incubated with horseradish peroxidase-conjugated goat anti-mus immunoglobulin G as the secondary antibody for 1 h at room temperature. After washing with TBST (150 mM NaCl, 0.1% Tween-20 in 20 mM Tris-HCl), the immunohistochemical reactions were visualised by using an Envision DAB kit (Dako, Tokyo, Japan). The sections were counterstained with haematoxylin. As a negative control for staining, the first antibodies were replaced with non-immune mouse immunoglobulin G (Dako). The sections were observed under a microscope (AxioImager A1; Carl Zeiss).

Lectin labelling of the retinal vasculature and adherent leucocytes

Leucocytes adhering to the retinal vasculature were imaged by perfusion labelling with fluorescein isothiocyanate-coupled concanavalin A lectin (Vector Laboratories, Burlingame, CA, USA).²⁷ After deep anaesthesia, the chest cavity was opened, a 20-gauge perfusion cannula was introduced into the aorta and a part of the liver was excised. After injection of 20 ml PBS to remove erythrocytes and non-adherent leucocytes, 20 ml of fluorescein isothiocyanate-conjugated concanavalin A lectin (40 μ g ml⁻¹) was injected. Residual unbound concanavalin A was removed with PBS perfusion. After the eyeballs were enucleated, the retina was flat-mounted and imaged under a fluorescence microscope (Axiovert 40; Carl Zeiss).

Enzyme-linked immunosorbent assay

To detect serum antibodies to the rAAV2 capsid and the transgenic protein, Chr2, we coated enhanced protein-binding enzyme-linked immunosorbent assay plates with 10⁹ viral particles per well of rAAV2 in 100 μ l of 0.1 M sodium carbonate buffer (pH 9.6) and with 0.2 μ g per well peptide coding for Chr2 by using a peptide coating kit (TaKaRa, Shiga, Japan) at 4 °C overnight. The wells were blocked with 10% fetal bovine serum-0.1% Tween in PBS for 30 min at

37 °C. Then, serum dilutions were added and incubated for 4 °C overnight. Dilutions of a rabbit anti-AAV2 capsid protein (American Research Product, Belmont, MA, USA) and a rabbit anti-Chr2 protein (TaKaRa) served as positive controls. The plates were incubated with horseradish peroxidase-conjugated anti-rabbit immunoglobulin G or anti-rat immunoglobulin G at 37 °C for 1 h in the presence of 3% goat serum. The reactions were visualised by adding one-step tetramethylbenzidine substrate (Promega, Tokyo, Japan). The reactions were stopped by adding 1 N HCl and read at 450 nm with a VERS Amax plate reader (Molecular Devices, Osaka, Japan). Each value was determined in triplicate.

Analysis of T lymphocytes

Peripheral blood CD4⁺ cells have a central role in regulating the cell-mediated immune response to infection. Often known as helper T cells, they act on other cells of the immune system to promote various aspects of the immune response, including immunoglobulin isotype switching and affinity maturation and enhanced activity of natural killer cells and cytotoxic T cells. CD4⁺ cells also act by releasing cytokines in response to antigenic stimulation. One of the major roles of CD4⁺ cells is the activation of macrophages. During the course of hepatitis C virus infection, two different immunological statuses can be observed. In the acute phase of infection, CD4⁺ helper T cells contribute to the induction and maintenance of a functional CD8⁺ cell response. In the chronic phase, T regulatory (CD4⁺CD25⁺) cells suppress CD8⁺ cell responses, and thereby help the virus to persist.⁴⁸ It is important to calculate these ratios to observe the immunological status.

Before and after the rAAV injection, peripheral blood was collected from the tail vein. Lymphocytes were isolated with PharmLyse (BD Bioscience, San Jose, CA, USA). After isolation, a mixture of monoclonal antibodies (mAbs) specific for CD3 (conjugated with Alexa Fluor 647; AbD Serotec, Oxford, UK), CD4 (conjugated with PE-Cy5; BD Bioscience), CD8a (conjugated with R-PE; BD Bioscience) and CD25 (conjugated with fluorescein isothiocyanate; BD Bioscience) was added to the cells, which were then incubated at 4 °C overnight. Flow-cytometric analysis was performed by using FACS Calibur (BD Bioscience) after washing the cells with PBS. For gating and calculation, CellQuest software (BD Bioscience) was used. In the FACS analysis, 10 000 cells were examined for each sample.

Statistical analysis

Statistical analysis was performed by using GraphPad Prism (GraphPad Software, San Diego, CA, USA). The criterion for statistical significance was $P < 0.05$ by Dunnett multiple comparison test.

CONFLICT OF INTEREST

The authors declare no conflict of interest.

ACKNOWLEDGEMENTS

This work was partly supported by Grants-in-Aid for Scientific Research from the Ministry of Education, Culture, Sports, Science and Technology of Japan (nos. 21791664 and 21200022); Science and Culture and Special Coordination Funds for Promoting Science and Technology of the Japanese Government, Strategic Research Programme for Brain Sciences (SRPBS); the Ministry of Health, Labour and Welfare of Japan; and Japan Foundation for Aging and Health and the Programme for Promotion of Fundamental studies in Health Sciences of the National Institute of Biomedical Innovation (NIBIO). I also thank Teru Hiroi for technical support in animal treatment.

- Hartong DT, Berson EL, Dryja TP. Retinitis pigmentosa. *Lancet* 2006; **368**: 1795–1809.
- Santos A, Humayun MS, de Juan Jr E, Greenburg RJ, Marsh MJ, Klock IB *et al*. Preservation of the inner retina in retinitis pigmentosa. A morphometric analysis. *Arch Ophthalmol* 1997; **115**: 511–515.
- Nagel G, Szellas T, Huhn W, Kateriya S, Adeishvili N, Berthold P *et al*. Channelrhodopsin-2, a directly light-gated cation-selective membrane channel. *Proc Natl Acad Sci USA* 2003; **100**: 13940–13945.

- 4 Bi A, Cui J, Ma YP, Olshevskaya E, Pu M, Dzhizhov AM *et al*. Ectopic expression of a microbial-type rhodopsin restores visual responses in mice with photoreceptor degeneration. *Neuron* 2006; **50**: 23–33.
- 5 Tomita H, Sugano E, Yawo H, Ishizuka T, Isago H, Narikawa S *et al*. Restoration of visual response in aged dystrophic RCS rats using AAV-mediated channelrhodopsin-2 gene transfer. *Invest Ophthalmol Vis Sci* 2007; **48**: 3821–3826.
- 6 Lagali PS, Balya D, Awatramani GB, Munch TA, Kim DS, Busskamp V *et al*. Light-activated channels targeted to ON bipolar cells restore visual function in retinal degeneration. *Nat Neurosci* 2008; **11**: 667–675.
- 7 Tomita H, Sugano E, Isago H, Hiroi T, Wang Z, Ohta E *et al*. Channelrhodopsin-2 gene transduced into retinal ganglion cells restores functional vision in genetically blind rats. *Exp Eye Res* 2010; **90**: 429–436.
- 8 Ishizuka T, Kakuda M, Araki R, Yawo H. Kinetic evaluation of photosensitivity in genetically engineered neurons expressing green algae light-gated channels. *Neurosci Res* 2006; **54**: 85–94.
- 9 Wang H, Peca J, Matsuzaki M, Matsuzaki K, Noguchi J, Qiu L *et al*. High-speed mapping of synaptic connectivity using photostimulation in Channelrhodopsin-2 transgenic mice. *Proc Natl Acad Sci USA* 2007; **104**: 8143–8148.
- 10 Tomita H, Sugano E, Fukazawa Y, Isago H, Sugiyama Y, Hiroi T *et al*. Visual properties of transgenic rats harboring the channelrhodopsin-2 gene regulated by the thy-1.2 promoter. *PLoS One* 2009; **4**: e7679.
- 11 Monville C, Torres E, Thomas E, Scarpini CG, Muhith J, Lewis J *et al*. HSV vector-delivery of GDNF in a rat model of PD: partial efficacy obscured by vector toxicity. *Brain Res* 2004; **1024**: 1–15.
- 12 Aiuti A, Bachoud-Lévi AC, Blesch A, Brenner MK, Cattaneo F, Chiocchia EA *et al*. Progress and prospects: gene therapy clinical trials (part 2). *Gene Therapy* 2007; **14**: 1555–1563.
- 13 Alexander BL, Ali RR, Alton EW, Bainbridge JW, Braun S, Cheng SH *et al*. Progress and prospects: gene therapy clinical trials (part 1). *Gene Ther* 2007; **14**: 1439–1447.
- 14 Thomas CE, Ehrhardt A, Kay MA. Progress and problems with the use of viral vectors for gene therapy. *Nat Rev Genet* 2003; **4**: 346–358.
- 15 Koizumi K, Poulaki V, Doehmen S, Welsandt G, Radetzky S, Lappas A *et al*. Contribution of TNF- α to leukocyte adhesion, vascular leakage, and apoptotic cell death in endotoxin-induced uveitis *in vivo*. *Invest Ophthalmol Vis Sci* 2003; **44**: 2184–2191.
- 16 Zhang YC, Powers M, Wasserfall C, Brusko T, Song S, Flotte T *et al*. Immunity to adeno-associated virus serotype 2 delivered transgenes imparted by genetic predisposition to autoimmunity. *Gene Therapy* 2004; **11**: 233–240.
- 17 Damoiseaux JG, Cautain B, Bernard I, Mas M, van Breda Vriesman PJ, Druet P *et al*. A dominant role for the thymus and MHC genes in determining the peripheral CD4/CD8 T cell ratio in the rat. *J Immunol* 1999; **163**: 2983–2989.
- 18 Kim SA, Lim SS. T lymphocyte subpopulations and interleukin-2, interferon- γ , and interleukin-4 in rat pulpitis experimentally induced by specific bacteria. *J Endod* 2002; **28**: 202–205.
- 19 Toda A, Piccirillo CA. Development and function of naturally occurring CD4+CD25+ regulatory T cells. *J Leukoc Biol* 2006; **80**: 458–470.
- 20 Simpson E. A historical perspective on immunological privilege. *Immunol Rev* 2006; **213**: 12–22.
- 21 Caldwell RB, McLaughlin BJ. Permeability of retinal pigment epithelial cell junctions in the dystrophic rat retina. *Exp Eye Res* 1983; **36**: 415–427.
- 22 Caldwell RB, McLaughlin RJ, Boykins LG. Intramembrane changes in retinal pigment epithelial cell junctions of the dystrophic rat retina. *Invest Ophthalmol Vis Sci* 1982; **23**: 305–318.
- 23 Caldwell RB, Wade LA, McLaughlin BJ. A quantitative study of intramembrane changes during cell junctional breakdown in the dystrophic rat retinal pigment epithelium. *Exp Cell Res* 1984; **150**: 104–117.
- 24 Chang CW, DeFoe DM, Caldwell RB. Retinal pigment epithelial cells from dystrophic rats form normal tight junctions *in vitro*. *Invest Ophthalmol Vis Sci* 1997; **38**: 188–195.
- 25 Nakai H, Yant SR, Storm TA, Fuess S, Meuse L, Kay MA. Extrachromosomal recombinant adeno-associated virus vector genomes are primarily responsible for stable liver transduction *in vivo*. *J Virol* 2001; **75**: 6969–6976.
- 26 Niemeyer GP, Herzog RW, Mount J, Arruda VR, Tillson DM, Hathcock J *et al*. Long-term correction of inhibitor-prone hemophilia B dogs treated with liver-directed AAV2-mediated factor IX gene therapy. *Blood* 2009; **113**: 797–806.
- 27 Satofuka S, Ichihara A, Nagai N, Yamashiro K, Koto T, Shinoda H *et al*. Suppression of ocular inflammation in endotoxin-induced uveitis by inhibiting nonproteolytic activation of prorenin. *Invest Ophthalmol Vis Sci* 2006; **47**: 2686–2692.
- 28 Reichelt W, Dettmer D, Bruckner G, Brust P, Eberhardt W, Reichenbach A. Potassium as a signal for both proliferation and differentiation of rabbit retinal (Muller) glia growing in cell culture. *Cell Signal* 1989; **1**: 187–194.
- 29 Hartig W, Grosche J, Distler C, Grimm D, el-Hifnawi E, Reichenbach A. Alterations of Muller (glial) cells in dystrophic retinæ of RCS rats. *J Neurocytol* 1995; **24**: 507–517.
- 30 Hao LY, Hao XQ, Li SH, Li XH. Prenatal exposure to lipopolysaccharide results in cognitive deficits in age-increasing offspring rats. *Neuroscience* 2010; **166**: 763–770.
- 31 Beurel E, Jope RS. Lipopolysaccharide-induced interleukin-6 production is controlled by glycogen synthase kinase-3 and STAT3 in the brain. *J Neuroinflammation* 2009; **6**: 9.
- 32 Ni YQ, Gan DK, Xu HD, Xu GZ, Da CD. Neuroprotective effect of transcorneal electrical stimulation on light-induced photoreceptor degeneration. *Exp Neurol* 2009; **219**: 439–452.
- 33 Morimoto T, Miyoshi T, Sawai H, Fujikado T. Optimal parameters of transcorneal electrical stimulation (TES) to be neuroprotective of axotomized RGCs in adult rats. *Exp Eye Res* 2010; **90**: 285–291.
- 34 Wang J, Jiang S, Kwong JM, Sanchez RN, Sadun AA, Lam TT. Nuclear factor-kappaB p65 and upregulation of interleukin-6 in retinal ischemia/reperfusion injury in rats. *Brain Res* 2006; **1081**: 211–218.
- 35 Kaltschmidt C, Kaltschmidt B, Neumann H, Wekerle H, Baeuerle PA. Constitutive NF-kappa B activity in neurons. *Mol Cell Biol* 1994; **14**: 3981–3992.
- 36 O'Neill LA, Kaltschmidt C. NF-kappa B: a crucial transcription factor for glial and neuronal cell function. *Trends Neurosci* 1997; **20**: 252–258.
- 37 O'Garra A, Vieira P. Regulatory T cells and mechanisms of immune system control. *Nat Med* 2004; **10**: 801–805.
- 38 Sakaguchi S. Regulatory T cells: key controllers of immunologic self-tolerance. *Cell* 2000; **101**: 455–458.
- 39 Shevach EM. CD4+ CD25+ suppressor T cells: more questions than answers. *Nat Rev Immunol* 2002; **2**: 389–400.
- 40 Li W, Asokan A, Wu Z, Van Dyke T, DiPrimio N, Johnson JS *et al*. Engineering and selection of shuffled AAV genomes: a new strategy for producing targeted biological nanoparticles. *Mol Ther* 2008; **16**: 1252–1260.
- 41 Koga T, Koshiyama Y, Gotoh T, Yonemura N, Hirata A, Tanihara H *et al*. Coinduction of nitric oxide synthase and arginine metabolic enzymes in endotoxin-induced uveitis rats. *Exp Eye Res* 2002; **75**: 659–667.
- 42 Kügler S, Lingor P, Schöll U, Zolotukhin S, Bähr M. Differential transgene expression in brain cells *in vivo* and *in vitro* from AAV-2 vectors with small transcriptional control units. *Virology* 2003; **311**: 89–95.
- 43 Auricchio A, Hildinger M, O'Connor E, Gao GP, Wilson JM. Isolation of highly infectious and pure adeno-associated virus type 2 vectors with a single-step gravity-flow column. *Hum Gene Ther* 2001; **12**: 71–76.
- 44 Auricchio A, O'Connor E, Hildinger M, Wilson JM. A single-step affinity column for purification of serotype-5 based adeno-associated viral vectors. *Mol Ther* 2001; **4**: 372–374.
- 45 Sugano E, Tomita H, Ishiguro S, Abe T, Tamai M. Establishment of effective methods for transducing genes into iris pigment epithelial cells by using adeno-associated virus type 2. *Invest Ophthalmol Vis Sci* 2005; **46**: 3341–3348.
- 46 Papatheanasiou ES, Peachey NS, Goto Y, Neafsey EJ, Castro AJ, Kartje GL. Visual cortical plasticity following unilateral sensorimotor cortical lesions in the neonatal rat. *Exp Neurol* 2006; **199**: 122–129.
- 47 Iwamura Y, Fujii Y, Kamei C. The effects of certain H(1)-antagonists on visual evoked potential in rats. *Brain Res Bull* 2003; **61**: 393–398.
- 48 Boettler T, Spangenberg HC, Neumann-Haefelin C, Panther E, Urbani S, Ferrari C *et al*. T cells with a CD4+CD25+ regulatory phenotype suppress *in vitro* proliferation of virus-specific CD8+ T cells during chronic hepatitis C virus infection. *J Virol* 2005; **79**: 7860–7867.

Dissecting a Role for Melanopsin in Behavioural Light Aversion Reveals a Response Independent of Conventional Photoreception

Ma'ayan Semo^{1*}, Carlos Gias¹, Ahmad Ahmado¹, Eriko Sugano², Annette E. Allen³, Jean M. Lawrence¹, Hiroshi Tomita², Peter J. Coffey¹, Anthony A. Vugler^{1*}

1 Department of Ocular Biology and Therapeutics, University College London-Institute of Ophthalmology, London, United Kingdom, **2** Institute for International Advanced Interdisciplinary Research, Tohoku University, Aoba-ku, Sendai, Japan, **3** Faculty of Life Sciences, University of Manchester, Manchester, United Kingdom

Abstract

Melanopsin photoreception plays a vital role in irradiance detection for non-image forming responses to light. However, little is known about the involvement of melanopsin in emotional processing of luminance. When confronted with a gradient in light, organisms exhibit spatial movements relative to this stimulus. In rodents, behavioural light aversion (BLA) is a well-documented but poorly understood phenomenon during which animals attribute salience to light and remove themselves from it. Here, using genetically modified mice and an open field behavioural paradigm, we investigate the role of melanopsin in BLA. While wildtype (WT), melanopsin knockout (*Opn4*^{-/-}) and *rd/rd cl* (melanopsin only (MO)) mice all exhibit BLA, our novel methodology reveals that isolated melanopsin photoreception produces a slow, potentiating response to light. In order to control for the involvement of pupillary constriction in BLA we eliminated this variable with topical atropine application. This manipulation enhanced BLA in WT and MO mice, but most remarkably, revealed light aversion in triple knockout (TKO) mice, lacking three elements deemed essential for conventional photoreception (*Opn4*^{-/-} *Gnat1*^{-/-} *Cnga3*^{-/-}). Using a number of complementary strategies, we determined this response to be generated at the level of the retina. Our findings have significant implications for the understanding of how melanopsin signalling may modulate aversive responses to light in mice and humans. In addition, we also reveal a clear potential for light perception in TKO mice.

Citation: Semo M, Gias C, Ahmado A, Sugano E, Allen AE, et al. (2010) Dissecting a Role for Melanopsin in Behavioural Light Aversion Reveals a Response Independent of Conventional Photoreception. PLoS ONE 5(11): e15009. doi:10.1371/journal.pone.0015009

Editor: Steven Barnes, Dalhousie University, Canada

Received: August 18, 2010; **Accepted:** October 11, 2010; **Published:** November 29, 2010

Copyright: © 2010 Semo et al. This is an open-access article distributed under the terms of the Creative Commons Attribution License, which permits unrestricted use, distribution, and reproduction in any medium, provided the original author and source are credited.

Funding: This work was funded by the London Project to Cure Blindness (www.thelondonproject.org/) and the Lincy Foundation. The funders had no role in study design, data collection and analysis, decision to publish, or preparation of the manuscript.

Competing Interests: The authors have declared that no competing interests exist.

* E-mail: a.vugler@ucl.ac.uk (AAV); m.semo@ucl.ac.uk (MS)

Introduction

In the 1920's, Crozier and Pincus showed that neonatal rats with closed eyelids will move away from bright light along a gradient towards a less intensely illuminated target [1]. Adult rats retain an aversion to light [2,3], so strong that it can be used as a motivating factor in behavioural learning paradigms [4]. Like rats, adult mice also show behavioural light aversion (BLA) to acute (10–30 mins) light exposure in the open field [5,6]. Using mice, the "light/dark box test" has been employed extensively in drug development to identify putative anxiolytic compounds (see [5], reviewed in [7]) and more recently to investigate human photophobia in mouse models of migraine [8,9]. Despite the widespread application of this behavioural phenomenon, and its undoubted importance to the lives of nocturnal animals, little is known about the neural circuitry mediating BLA in rodents. Although one study to date has implicated both subcortical and cortical processing [10], the contribution of different photoreceptive components from the retina remains unclear.

In the mammalian retina, rods/cones of the outer retina are known to mediate image-forming vision [11,12], while photoreceptive melanopsin-expressing retinal ganglion cells (mRGCs) of

the inner retina sub serve most non-image-forming responses to light [13,14,15,16,17]. If the eyes are enucleated bilaterally, then BLA in rats is abolished [10]. To date, only a few studies shed light on the important question of whether melanopsin alone could mediate this primitive non-image-forming response. These studies, from a variety of animal models, report mixed conclusions about a potential role for melanopsin in BLA.

A recent study investigating the role of melanopsin in non-image forming functions found that targeted destruction of melanopsin cells had no impact on the light:dark preference of mice [18]. This is in line with data from RCS rats showing a progressive loss of BLA over time, with no response detectable by 7 months [19]. Another study using *rd* mice also failed to report a significant light aversion response following exposure to illumination of 2800 Lux [20].

In contrast, spatial responses to light have been reported in *rd* mice given the choice between light and dark living/nesting areas over a 22 h period [21]. Here, retinal degenerate mice spent significantly more time in the dark than the illuminated area, a response that could be eliminated by enucleation. However, as *rd* mice retain a significant population of remodelled cones with identifiable presynaptic structures [22,23,24,25] they are unsatisfac-

tory for defining a role for melanopsin in BLA. In the present study we employ the *rd/rd cl* mouse, which lacks both rods and cones [15].

Melanopsin is a retinaldehyde-based, invertebrate-like photopigment [26,27] involved with mediating many responses to light that require a measure of general environmental irradiance [14,15,28,29,30] and more recently, the ability of light to modulate sleep [31,32,33]. Importantly, an associative learning (Pavlovian conditioning) paradigm has shown that *rd/rd cl* mice can gradually learn to use a brief light stimulus to predict the onset of electric shocks [34]. Although melanopsin cells are thought to project mainly to subcortical, non-image forming centres of the brain, they may also signal luminance information to the visual cortex [35,36,37,38].

In humans, light aversion is often referred to as photophobia, a clinical term describing pain onset following light exposure in a number of conditions including migraine headache [39,40,41]. Recently, the melanopsin system has been implicated in the potentiation of migraine by light in blind patients [42] and although little is known about the neural circuitry of photophobia it is generally considered to require a convergence of information from optic and trigeminal nerves with associated cortical processing [40,42,43,44]. In addition, because sensory trigeminal afferents innervate muscles of the iris, sustained constriction caused by the pupillary light reflex (PLR) has also been implicated in causing the ocular discomfort felt following exposure to bright lights [40,41,45]. The term photophobia is also used to describe the sensation felt when we, as humans, enter an environment which is subjectively appraised as being “too bright”, eliciting aversive behavioural responses such as looking away from bright light and squinting [46,47,48].

Our goal in the present study was to determine the extent to which melanopsin mediates BLA in mice. To achieve this, we developed a variation on an established protocol for measuring light aversion in mice [6], which now takes into account the behaviour of animals placed into complete darkness. We tested naïve wildtype (WT) mice, *rd/rd cl* mice (hereafter referred to as melanopsin only (MO)) [14,31], melanopsin knockout (MKO) mice (*Opn4^{-/-}*) [30] and as a control for the absence of light perception, triple knockout (TKO) mice, lacking melanopsin and functional rods/cones (*Opn4^{-/-} Gnat1^{-/-} Cnga3^{-/-}*). These mice have no significant PLR, circadian photoentrainment or masking responses [49]. In order to investigate if pupillary constriction is causally related to BLA, we also equalised this variable across genotypes by applying atropine bilaterally to the eyes.

Our experiments show that melanopsin alone can mediate a behavioural aversion to light that is associated with neural activation in the extended visual cortex. Analysis of temporal kinetics reveals that melanopsin acts slowly to increase light aversion over time, whereas rods/cones drive a more immediate aversive response. While MKO mice remain capable of BLA our analysis reveals that rods/cones and melanopsin are required for an aversive response characteristic of WT animals. Surprisingly, the addition of atropine increased BLA in WT, MO and TKO mice, with this new light perception in TKO's being associated with an enhancement of residual retinal activity. The retinal origin of light aversion behaviour in TKO mice was further investigated by either eliminating BLA with bilateral axotomy or generating a response comparable to that seen in wildtype animals by specifically activating retinal neurons using *Channelrhodopsin-2*.

Results

Melanopsin alone can drive the behavioural aversion to light

Animals were tested for BLA for 30 minutes in the open field apparatus shown in Figure 1A. This behaviour was assessed by

comparing time spent in the dark back-half (BH) when the front-half (FH) was illuminated (light FH) with control conditions when the FH was maintained in darkness (dark FH).

Over the whole trial, WT normally-sighted animals spend the majority of their time (67%) in the dark BH of the arena when the FH is illuminated (Figure 1B). This is also significantly more time ($p < 0.001$) than when the FH is maintained in darkness during which they spend only 34% of the time in the BH. The *rd/rd cl* animals, with only melanopsin as a functional photopigment (MO) do not spend the majority of their time in the dark when the FH is illuminated (46%), however a significant light-aversion response is revealed when this is compared to the amount of time that is spent in the BH when there is no illumination (27%) ($p < 0.01$).

This result, together with previous observations of an impairment to BLA following lesions of visual cortex [10] prompted us to examine if melanopsin alone could drive activation of this structure in mice. This was achieved by examining light-induced c-Fos in the visual cortex of MO animals, a technique previously validated for normally sighted mice [50]. Here, using the same light source as that used for behavioural testing, we found a clear, melanopsin-driven c-Fos induction in medial visual/retrosplenial cortex (Figure S1).

Melanopsin is not required for the behavioural aversion to light

As seen in Figure 1, rods/cones also play a major role in BLA. When the behaviour of the congenic MO and WT mice are compared by two-way ANOVA there is a significant effect of genotype ($p < 0.01$) and of light ($p < 0.0001$), with Bonferroni's multiple comparison tests confirming a significant reduction in time spent in the dark BH when the FH is illuminated in the MO (46%) compared to the WT (67%) mice ($p < 0.01$). In control conditions, when the entire arena is in darkness there is no significant difference in behaviour between MO and WT mice, both seeming to retain a preference for the FH.

Animals lacking melanopsin (MKO) spend significantly more time (60%, $p < 0.05$) in the dark BH when light is on in the FH (Figure 1B), than when there is no illumination (only 28% of time spent in BH). This finding shows that although melanopsin alone can mediate BLA, the presence of this photopigment is not a requirement for this response to occur. As anticipated, in TKO mice (lacking melanopsin and normal rod/cone function), there is no response to illumination in the FH, with these mice spending similar amounts of time ($p > 0.05$) in the BH whether the FH is in darkness or light (29 versus 21% of the time).

Interestingly, regardless of whether the light was on or off, TKO mice spend most of their time in the open FH of the arena, as do the other genotypes in the complete darkness control condition. This phenomenon holds true regardless of which side of the arena animals are first placed (data not shown). To the best of our knowledge, this consistent behaviour has not been reported previously and should be taken into account when interpreting data derived from light:dark choice tests of a similar design to ours.

Temporal kinetics of light aversion in mice

To investigate the behaviour of mice during the course of the 30-minute trial, data were binned into 6, 5-minute bins throughout the trial (Figure 2A–D). Results of the associated regression analysis are summarised in table 1. Under control conditions (complete darkness), in all genotypes, animals failed to change the amount of time spent in the BH (slopes of regression lines are not significantly non-zero). However, when there is light in the FH of the arena, both WT and MO mice show a positive correlation with duration of the trial, spending more time in the

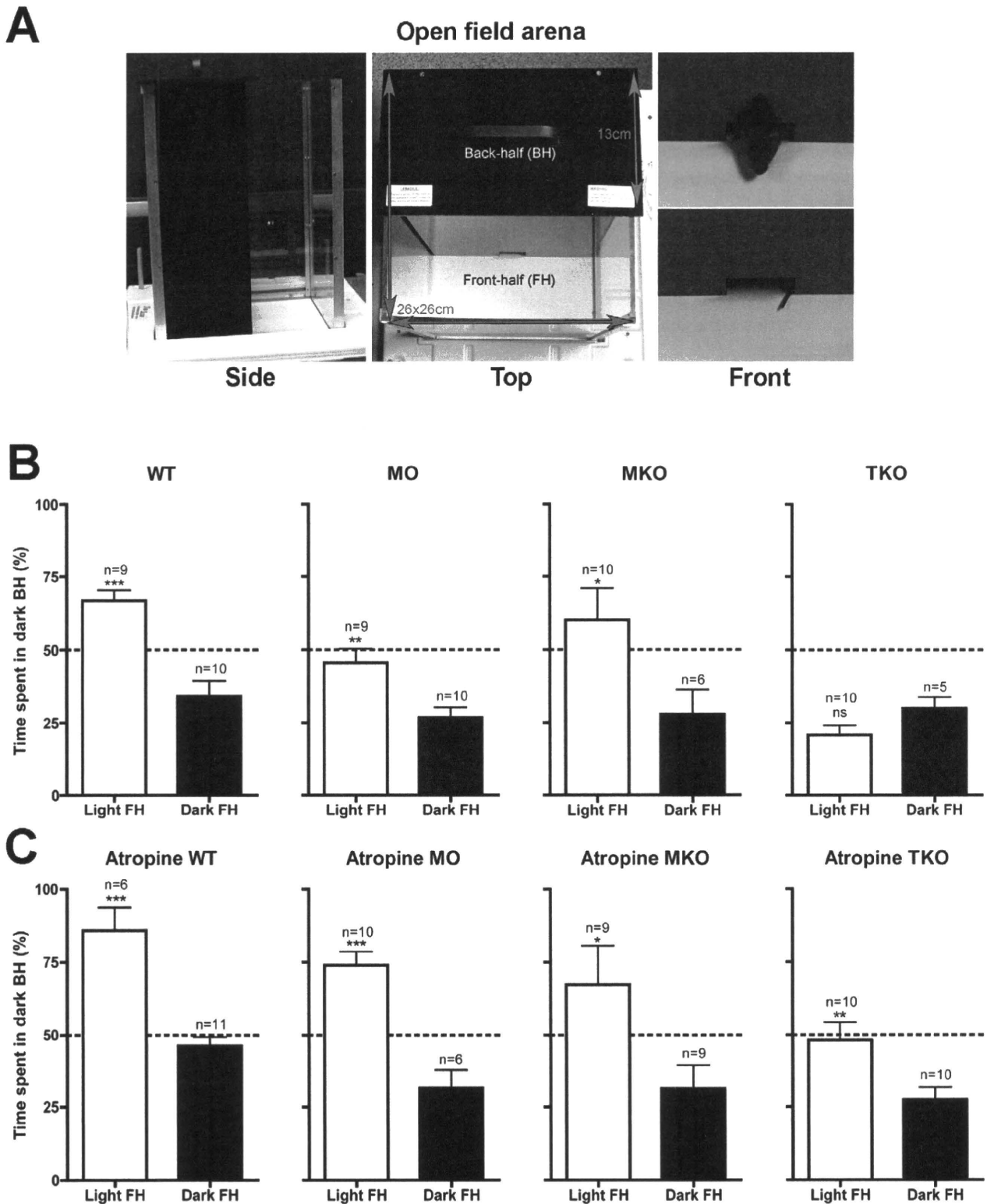


Figure 1. Role of melanopsin in the behavioural aversion to light in mice. (A) Open field apparatus: animals were placed into the front-half (FH) of the arena and remained there for 30 minutes. Time spent in the back-half (BH) of the arena was recorded. (B) and (C) Average (\pm SEM) percentage of time spent in the dark BH of the arena during the 30-minute trial. The FH is either illuminated, white bars (light FH), or in darkness, black bars (dark FH). (B) In untreated animals photophobic behaviour is evident in wildtype (WT), melanopsin only (MO) *rd/rd cl* mice, and melanopsin knockout (MKO) mice. Triple knockout (TKO) mice, lacking melanopsin and functional rods and cones show no aversion to light. (C) Atropine significantly increases aversive behaviour in WT, MO, and TKO mice. In MKO mice, atropine increases the average aversive behaviour but this does not reach significance. Atropine does not significantly affect behaviour when the FH is in darkness in any of the genotypes. Stars (*) indicate significance levels (Student's *t*-test): * $p < 0.05$; ** $p < 0.01$; *** $p < 0.001$. doi:10.1371/journal.pone.0015009.g001

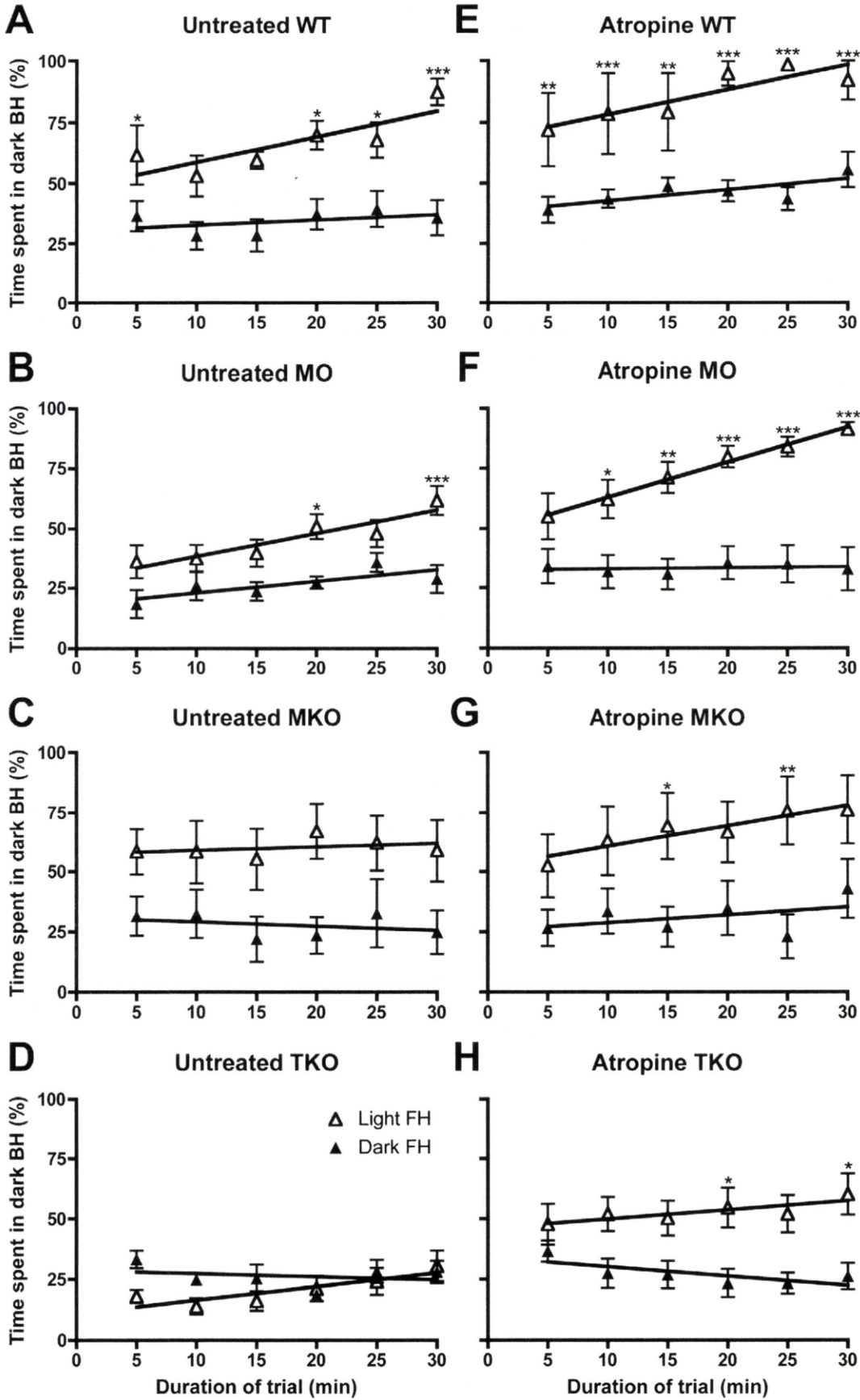


Figure 2. Temporal kinetics of the behavioural aversion to light in mice. Graphs showing time spent in the dark back-half (BH) of the arena over the course of the 30-minute trial. Data are binned into 6, 5-minute bins throughout the trial, with y-axis showing average (\pm SEM) percentage time spent in the dark BH. (A–D) shows data from untreated animals, and (E–H) after bilateral application of atropine drops. (A) and (E) WT, (B) and (F) MO (*rd/rd cl*), (C) and (G) MKO (*Opn4^{-/-}*) and (D) and (H) TKO (*Opn4^{-/-} Gnat1^{-/-} Cnga3^{-/-}*). White triangles, trials when the front-half (FH) is in light, black triangles, trials when the FH is in darkness. Results of the regression analyses are shown in table 1. Stars (*) indicate significance levels (Bonferroni post tests, light FH v dark FH at each time point): * $p < 0.05$; ** $p < 0.01$; *** $p < 0.001$. doi:10.1371/journal.pone.0015009.g002

dark BH in the last 5 minutes. To compare the effect of the light to control conditions over the course of the trial, two-way repeated measures ANOVA (RM ANOVA) was carried out on data from each genotype, the results of Bonferroni post-tests are indicated on the graphs in Figure 2.

The WT (Figure 2A) and MO (Figure 2B) mice show a similar pattern of behaviour over the course of the trial, with the RM ANOVA test revealing a significant effect of time (WT $p < 0.01$, MO $p < 0.001$), light (WT $p < 0.001$, $p < 0.01$) and an interaction between time X light (WT $p < 0.05$, MO $p < 0.05$). In the last 5 minutes of the trial (minutes 25–30) the WTs and MOs spend the highest proportion of their time in the dark (87% WTs and 62% MOs). It is however clear when comparing the behaviour of WTs and MOs that melanopsin does not mediate all aspects of normal light aversion behaviour. Unlike MOs, the WT mice show a significant aversive response during the first 5 minutes of the trial and spend a higher proportion of their time in the dark BH.

As shown in Figure S2, aged MO animals retain their BLA, despite a well-documented loss of melanopsin cells with advancing age in these animals [51,52]. Interestingly, aging alters the behaviour of MO mice over the duration of the trial, so that during the first 5 minutes of the trial light aversion is intensified in older MOs compared to younger animals (Figure S2B). This result is of note and implies an increase in the potency of melanopsin signalling in retinal dystrophy with advancing age.

In MKO mice we found no significant correlation with duration of the trial and time spent in the dark BH. From the beginning to the end of the trial these mice spent 60% of their time in the back-half, similar to their overall average (Figure 2C). For this group of mice RM ANOVA showed a significant effect of light ($p < 0.05$), but not for duration of trial or the interaction term light X time. As expected, the TKO mice did not display a significant aversion to light, with RM ANOVA showing no significant effect of light, time or the interaction term, with no differences between light FH and dark FH by Bonferroni post-tests. However, rather curiously, over the 30-minute trial duration, TKO mice do show a positive correlation with respect to the amount of time spent in the dark BH of the arena when the FH is illuminated (see Figure 2D and table 1).

In summary, when rods and cones are absent, melanopsin is capable of driving a slower onset BLA that is only clearly revealed after 15–20 minutes. Conversely, in the absence of melanopsin, animals retaining significant light aversion lack the positive correlation over time. Animals lacking melanopsin and properly functioning rods and cones (TKO) do not exhibit significant light aversion. Therefore, in order to display the aversion to light characteristic of their species, rodents must possess rods/cones and the photopigment melanopsin.

Ocular application of atropine enhances light aversion

In order to investigate the impact of eliminating the variable of pupillary constriction on BLA, atropine drops were applied

Table 1. Regression analysis of temporal kinetics of light aversion in mice.

Genotype	Treatment	Significant non-zero slope (p)	r^2	Slope
WT	Light Untreated	<0.05	0.68	1.05 \pm 0.36
WT	Dark Untreated	>0.05	-	-
MO	Light Untreated	<0.01	0.86	0.97 \pm 0.20
MO	Dark Untreated	>0.05	-	-
MKO	Light Untreated	>0.05	-	-
MKO	Dark Untreated	>0.05	-	-
TKO	Light Untreated	<0.05	0.75	0.56 \pm 0.16
TKO	Dark Untreated	>0.05	-	-
WT	Light Atropine	<0.05	0.78	1.01 \pm 0.27
WT	Dark Atropine	>0.05	-	-
MO	Light Atropine	<0.0001	0.99	1.46 \pm 0.07
MO	Dark Atropine	>0.05	-	-
MKO	Light Atropine	<0.01	0.87	0.88 \pm 0.17
MKO	Dark Atropine	>0.05	-	-
TKO	Light Atropine	<0.05	0.70	0.38 \pm 0.12
TKO	Dark Atropine	>0.05	-	-
TKO	Light Axotomy/Atropine	>0.05	-	-
TKO	Dark Axotomy/Atropine	>0.05	-	-
TKO	Light AAV2-ChR2V	<0.05	0.66	0.78 \pm 0.28

doi:10.1371/journal.pone.0015009.t001

bilaterally to the eyes 30 minutes prior to placing naïve animals into our open field arena. Other mydriatics were tested initially (e.g. phenylephrine, and tropicamide), however these agents were found to be either too short acting for the 30-minute trial and/or to cause mild distress, as such they were deemed unsuitable for use in combination with behavioural testing. Atropine on the other hand was ideal for this experiment as it relaxes the circular muscles of the iris to cause a painless and long-lasting mydriasis [53].

The application of atropine to the eyes of experimental animals produced no outward signs of discomfort and resulted in sustained pupil dilation. Figure 3A shows the PLR of MO mice to white light illumination (intensity-matched to that found in the experimental arena), following atropine application, the pupil no longer constricts. Unlike the other three genotypes tested here, TKO mice already lack pupil constriction, with neither atropine nor illumination able to change their pupil area (Figure 3B). It should be noted that the constriction mechanism itself in TKO mice remains intact, as demonstrated previously by application of the parasympathetic agonist carbachol [49].

As shown in Figure 1C, when atropine is applied prior to testing, all genotypes (including TKO mice) exhibit significant BLA, spending more time in the dark BH when the FH is illuminated. The influence of light and atropine in each genotype was assessed by two-way ANOVA followed by Bonferroni's multiple comparison tests. In the WT and MO there is a significant effect of light (WT, $p < 0.001$; MO $p < 0.001$) and atropine (WT, $p < 0.001$; MO, $p < 0.01$), there is also a significant interaction between light X atropine only in MO (WT, not significant; MO $p < 0.05$). *Post hoc* tests reveal that with atropine

application, light aversion is significantly increased ($p < 0.01$) from 67% to 86% in WT's, and from 46% to 74% ($p < 0.001$) in MO's. Atropine did not have a significant effect on behaviour in the dark in either the WT's or MO's.

Comparing the WT and MO behaviour by two-way ANOVA (factors: light and genotype) there is still an effect of both light ($p < 0.0001$) and genotype ($p < 0.05$) but by *post hoc* comparison testing the MO is no longer significantly less light averse than the WT as was the case in the non atropine treated animals. Atropine application is therefore greatly enhancing melanopsin-mediated BLA, such that MO's lacking rods and cones are now behaving much more like WT animals. By contrast, in MKO mice atropine does not significantly enhance light aversion (Figure 2C), with two-way ANOVA revealing a significant effect of light ($p < 0.01$) but not of atropine. In these animals, *post hoc* testing confirms there is no statistically significant change in light aversion with atropine application when either the FH is illuminated or in control conditions when the entire arena is in darkness.

Rather surprisingly, two-way ANOVA reveals a significant effect of atropine ($p < 0.05$) and a significant interaction between light and atropine ($p < 0.05$) in the TKO mice. *Post hoc* testing confirms that there is a significant increase in light aversion behaviour with the application of atropine ($p < 0.01$) from 21% to 53% of time spent in the dark BH when the light is on. Again, atropine had no influence on behaviour in control conditions when the FH is in darkness.

Following atropine application, all the genotypes now show a positive correlation over the course of the trial spending more time in the dark BH as the trial progresses when the FH is illuminated

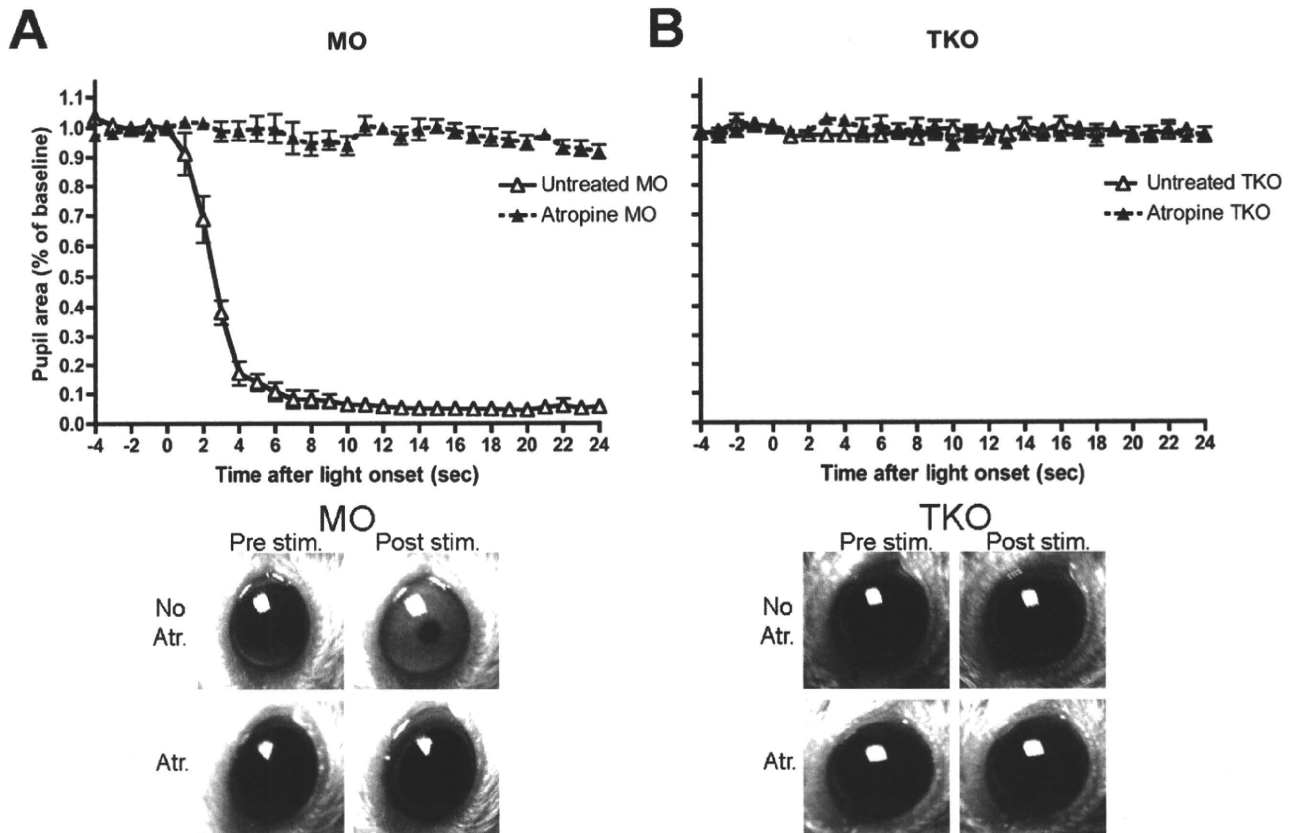


Figure 3. Effect of atropine on pupil size. In (A) MO (*rd/rd cl*), and (B) TKO (*Opn4^{-/-} Gnat1^{-/-} Cnga3^{-/-}*) mice. Images below each graph illustrate pupil size pre- and post- light stimulation with atropine (Atr.) or without atropine (No Atr.) application in the two genotypes. doi:10.1371/journal.pone.0015009.g003

(Figure 2E–H; table 1). In the last 5 minutes of the light FH trial, WT mice spend 92% of the time in the dark BH, and at this point the MO is almost indistinguishable, spending 91% of the time in the dark. The MKO also spends most time in the dark at this point (76%), and surprisingly the TKO also exhibits quite a striking aversion to light, spending 60% of the time in the dark in the final 5 minutes of the trial. Two-way RM ANOVA of atropine treated WT (Figure 2E), MO (Figure 2F), and MKO (Figure 2G), behaviour reveals a significant effect of time (WT, $p < 0.01$; MO, $p < 0.0001$; MKO, $p < 0.001$) light (WT, $p < 0.001$; MO $p < 0.001$; MKO, $p < 0.001$) and an interaction between time X light (WT, $p < 0.05$; MO, $p < 0.01$; MKO $p < 0.01$). The two-way RM ANOVA on atropine treated TKO mice (Figure 2H) shows there to be a significant effect of light ($p < 0.05$) and a significant interaction between light X time ($p < 0.05$) on BLA. It is clear that towards the end of the trial, TKO mice now spend significantly more time in the dark BH when the light is on in the FH than in control conditions with the dark FH.

The mechanism by which atropine is increasing light aversion in TKO mice is not readily apparent. In the other three genotypes (WT, MO and MKO), atropine application is causing pupil dilation and as such, their enhanced behavioural response could be attributed to more light entering the eye. However, in TKO mice this cannot be the case as we found their pupils to be fully dilated regardless of atropine administration (Figure 3B). As such, atropine would appear to be enhancing some residual light perception retained in these animals. This may be at the level of the retina or, alternatively, through a more systemic route acting on more central components of the visual system. Indeed, recent work from the Lucas laboratory has identified a small but significant electrophysiological response to light, both at the level of the ERG and the dorsal lateral geniculate nucleus of the thalamus [54]. To test the hypothesis that atropine might be influencing responsiveness of the TKO retina directly we carried out ERG recordings on these mice with and without atropine. Atropine does indeed significantly enhance the b-wave amplitude in TKO mice (Figure 4).

Aversion to light in TKO mice is driven by signals from the retina

In order to determine if the atropine-enhanced BLA of TKO mice was being driven by signals from the retina (as opposed to a local-systemic action of this drug on the brain), we used two complementary approaches: 1. Eliminate retinal input to the brain using bilateral axotomy and 2. Specifically render retinal neurons light sensitive using a non-pharmacological agent (the microbial opsin *Channelrhodopsin-2* (*ChR2*)), unable to potentiate the function of more remote components of the visual system.

For axotomy, in order to minimise the trauma associated with established procedures [55,56], we developed a novel technique that uses an intraocular, sub-retinal approach (see diagram in Figure 5A). As shown in Figure 5B and Figure S3, at 9 days post-axotomy, our technique has obliterated calretinin-positive retinal axons innervating the brain, confirming successful axotomy.

As shown in Figure 5C, after axotomy and subsequent atropine application, TKO mice no longer show a significant light aversion response over the whole trial (light FH versus dark FH Student's *t*-test $p > 0.05$). Over the course of the trial there is also no correlation with the amount of time the animals spend in the dark BH with light FH or dark FH (see Figure 5D; Table 1). Also, Two-way RM ANOVA did not reveal any significant effects of light or trial duration on the time spent in the dark BH. These data show that axotomy abolishes the atropine-induced BLA in TKO mice.

In order to confirm that enhanced retinal output is sufficient to drive BLA in TKO mice, we rendered their retinæ directly light sensitive. This was achieved by transfecting inner retinal neurons with *ChR2* using an intravitreal injection of an adeno-associated viral vector (AAV), which causes *Channelrhodopsin-2/Venus* (*ChR2V*) fusion protein expression in the retinal ganglion cells [57,58]. The expression of *ChR2V* gene is under the control of the CAG promoter which results in approximately 30% of retinal ganglion cells expressing *ChR2* [58]. It has previously been demonstrated that the viral construct we use here (AAV2-*ChR2V*) restores visual responses in rodents with degenerate rods/cones, while the Venus fluorescent reporter alone (AAV2-*Venus*) does not [57,58].

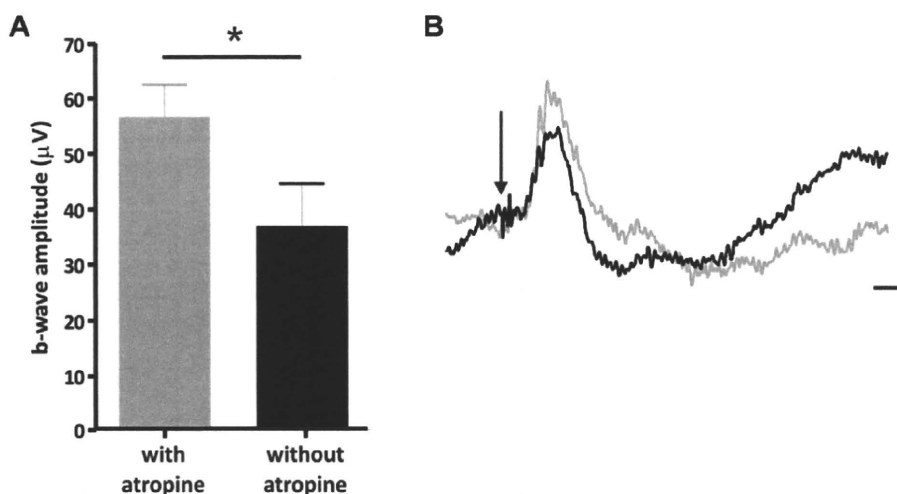


Figure 4. Atropine augments an ERG b-wave preserved in TKO mice. (A) b-wave amplitude of flash ERG responses in the presence and absence of atropine drops. A small but significant increase in the ERG b-wave amplitude was apparent following application of atropine drops (data presented as mean \pm SEM; $n = 5$ for each group). This is demonstrated in the average of all ERG responses in each group, shown in (B), atropine treated shown in grey, and untreated in black (scale bars: y-axis = 25 μ V, x-axis = 50 ms; $n = 5$ for each group).

doi:10.1371/journal.pone.0015009.g004

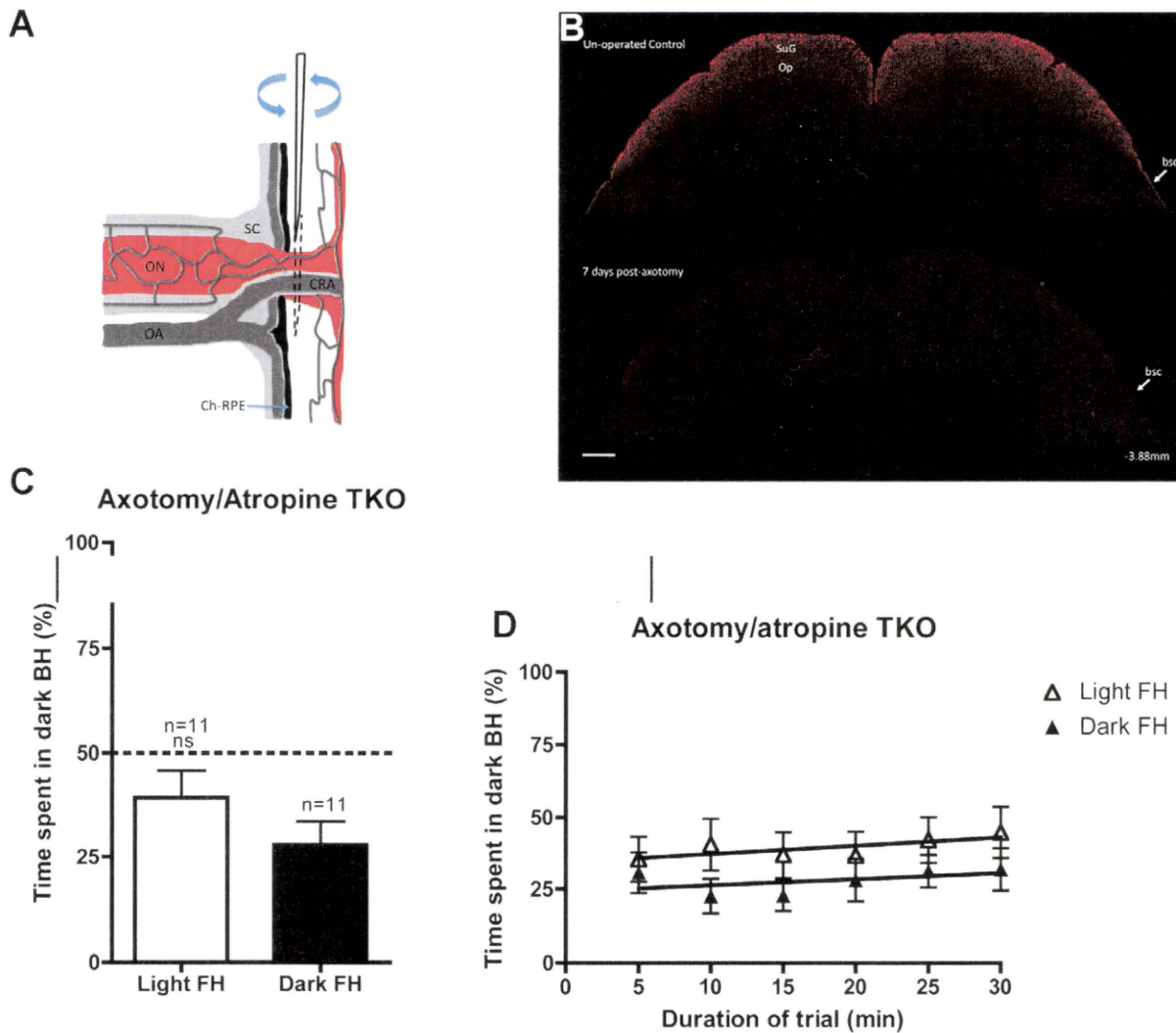


Figure 5. Axotomy abolishes the atropine-induced light aversion response in TKO mice. (A) Diagrammatic illustration of the axotomy technique (image modified from [75]), a swift back and forth movement of the needle severs both the optic nerve and central retinal artery. (B) Immunoreactivity for calretinin positive retinal afferents (red) is abolished in the superficial gray (SuG) and the optic nerve (Op) layers of the superior colliculus of a bilaterally axotomized TKO (bottom) compared to an unoperated control (top). Collicular sections are -3.88 mm from bregma [76], scale bar is $200\ \mu\text{m}$. (C) Behavioural aversion to light in atropine-treated TKO mice is abolished in bilaterally axotomized animals. (D) Time spent in the dark back half (BH) of the arena over the course of the 30-minute trial. White triangles, from trials when the front-half (FH) is in light, black triangles when the FH is in darkness. Abbreviations: bsc, brachium of the superior colliculus; Ch-RPE, choroid retinal pigment epithelium; CRA, central retinal artery; ns, not significant; OA, ophthalmic artery, ON, optic nerve; Sc, sclera.
doi:10.1371/journal.pone.0015009.g005

As shown in Figure 6, 2 months post-bilateral-injection of AAV2-*ChR2V* into adult TKO mice, cells across the entire inner retina were transduced to express ChR2V (green). In Figure 6B the red cells are stained for β -galactosidase, the reporter gene that replaces the melanopsin gene in TKO mice. Interestingly, by double-labelling in this fashion we very rarely encountered β -galactosidase positive cells that had been transduced to express the microbial opsin (<5 cells per retina).

As shown in Figure 6C, following ChR2V transduction, TKO mice (denoted AAV2-*ChR2V* TKO) now show an aversion to light similar to that of WT mice (WTs spend $67 \pm 4\%$ (mean \pm SEM) and AAV2-*ChR2V* TKOs spend $68 \pm 10\%$ (mean \pm SEM) in the dark back half when the front half is illuminated). The AAV2-*ChR2V* TKO mice also exhibit a positive correlation in their behaviour over the duration of the trial (Figure 6D), spending most time in the dark BH at the end of the trial (74%). Two-way RM

ANOVA comparing the untreated to AAV2-*ChR2V* treated TKOs reveals a significant effect of treatment ($p < 0.001$), and a significant effect of time ($p < 0.05$). Bonferroni post tests show that at all time points during the trial, AAV2-*ChR2V* TKOs are significantly more averse to light than the untreated animals in the light (Figure 6D). Importantly for addressing the role of pupillary constriction in BLA, the transduced mice exhibited this strong aversion to light in the absence of a detectable PLR (Figure S4).

Discussion

The photopigment melanopsin has an established role in non-image forming behavioural responses to light such as circadian photoentrainment, negative masking and the induction of sleep [15,28,31,32,33]. It has also been shown to be sufficient for the acquisition of a Pavlovian association between light and

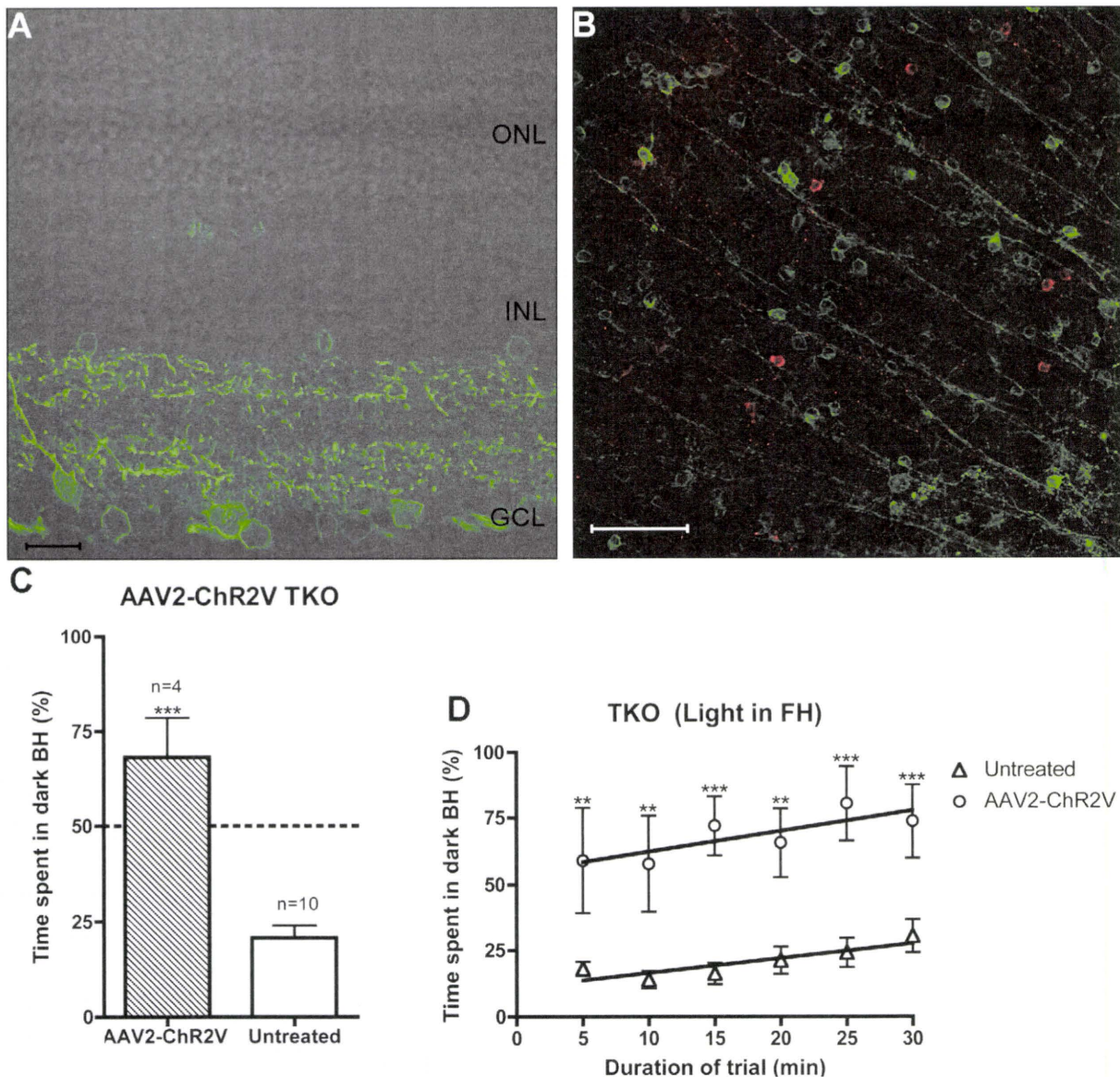


Figure 6. Channelrhodopsin-2 expression in the inner retina of TKO mice causes the induction of behavioural light aversion. (A) and (B) AAV2 transduced expression of Channelrhodopsin-2/Venus fusion (ChR2V) protein (green) in the ganglion cell layer of a TKO retina (AAV2-ChR2V TKO). (A) Transverse retinal section, ChR2V is visualised in many cells of the ganglion cell layer. Scale bar 20 μ m (B) Immunohistochemistry on flat mount retina (focussing on the ganglion cell layer) for β -galactosidase (red) with ChR2V in green. Scale bar 100 μ m. (C–D) Light aversion behaviour in the AAV2-ChR2V TKO. In these two graphs the comparison is between transduced and untreated animals when there is illumination in the front-half (FH). (C) Time spent in the dark back-half (BH) of the arena during the total 30 minutes of the trial. (D) Time spent in the dark (BH) of the arena over the course of the 30-minute trial. Stars (*) indicate significances (** $p < 0.01$; *** $p < 0.001$). doi:10.1371/journal.pone.0015009.g006

impending negative reinforcement [34]. Here, using naïve adult mice, we confirm a new and important role for melanopsin in the attribution of emotional salience to light. Quite unexpectedly, our investigations also reveal a capacity for light perception/BLA in mice lacking three components deemed necessary for photoreception.

Melanopsin mediates a slow behavioural aversion to light

As reported for normally sighted animals in previous studies, we found a clear aversion to light by WT mice within the first 5 minutes of our test. However, in MO mice, where melanopsin alone drives this response there is a slower, more gradual BLA

over time. The majority of light:dark testing paradigms used to date employ short trials (5–10 min duration) and we suggest that this may be one factor in the failure to report light aversion in previous studies using retinal degenerate rodents [19,20]. Our results are however consistent with those from a 22 h experiment suggesting a role for melanopsin in the preference displayed by *rd*/rod-ablated mice for a darkened nesting compartment [21]. Additionally, our data from MO mice shows that melanopsin-driven BLA has a strong positive correlation over time, potentiating light aversion over the course of our trial.

As with many other non-image forming responses to light, our data from MKO mice shows that melanopsin is not required for BLA to occur. However, these animals lack a positive correlation